

Genesis of the Calc-Alkaline Igneous Rock Suite

TREVOR H. GREEN and A. E. RINGWOOD

Department of Geophysics and Geochemistry, Australian National University, Canberra, A.C.T. Australia

Received January 25, 1968

Abstract. A high pressure experimental study of the partial melting fields of synthetic high-alumina olivine tholeiite, high-alumina quartz tholeiite, basaltic andesite, andesite, dacite and rhyodacite under dry and wet ($P_{H_2O} < P_{LOAD}$) conditions has been conducted in order to investigate possible origins of the calc-alkaline series from the upper mantle. Detailed analyses of crystallizing phases using the electron microprobe has enabled calculation of the liquid line of descent in these compositions at various pressures.

At 27—36 kb garnet and clinopyroxene are the liquidus or near-liquidus phases in dry tholeiite, basaltic andesite and andesite, while quartz is the liquidus phase in dry dacite and rhyodacite. Under wet conditions at 27 kb garnet, not quartz, is the liquidus phase in the dacite. Qualitatively these results show that the low melting fraction of a quartz eclogite at 27—36 kb under dry conditions is of andesitic composition whereas under wet conditions it is rhyodacitic or granodioritic. At these pressures under dry conditions the andesite liquidus lies in a marked low temperature trough between the more basic and more acid compositions. Quantitatively, the calculated compositions of liquid fractionates for varying degrees of melting of the quartz eclogite bulk composition broadly follow the calc-alkaline trend.

At 9—10 kb under wet conditions ($P_{H_2O} < P_{LOAD}$) sub-silicic amphibole and pyroxenes are the near-liquidus phases in tholeiite and basaltic andesite compositions. Calcic plagioclase and garnet occur nearer the solidus. The calculated liquid fractionates follow the calc-alkaline trend and demonstrate that the calc-alkaline series may be derived by the partial melting of amphibolite at lower crustal depths under wet conditions ($P_{H_2O} < P_{LOAD}$), or by the fractional crystallization of a hydrous basalt magma at similar depths.

These experimental results support two complementary hypotheses for the derivation of the calc-alkaline igneous rock suite from the mantle by a two stage igneous process. In the first stage of both hypotheses large piles of basalt are extruded on the earth's surface. Subsequently this pile of basalt may, under dry conditions, transform to quartz eclogite, sink into the mantle and finally undergo partial melting at 100—150 kms depth. This partial melting gives rise to the calc-alkaline magma series leaving a residuum of clinopyroxene and garnet. Alternatively, if wet conditions prevail in the basalt pile and the geotherms remain high, partial melting of the basalt may take place near the base of the pile, at about 10 kb pressure ($P_{H_2O} < P_{LOAD}$). The liquids so formed constitute the calc-alkaline suite and the residuum consists of amphibole, pyroxenes and possibly minor garnet and calcic plagioclase. Both models may be directly linked to the hypothesis of sea-floor spreading.

Contents

Introduction	106
Chemistry of the Calc-Alkaline Suite	106
Mineralogy of the Calc-Alkaline Suite	107
Hypotheses of Origin of the Calc-Alkaline Igneous Rock Suite	108
a) Fractional Crystallization of Basaltic Magma	108
b) Melting of Pre-Existing Sial, Hybridism or Mixing of Magmas	110
c) Contamination of Basaltic Magma with Sialic Crust	111
d) Partial Melting of Quartz Eclogite at 100—150 kms Depth	111
e) Partial Melting of Basalt at 30—40 kms Depth under Wet Conditions ($P_{H_2O} < P_{LOAD}$)	112

Experimental	114
Analytical	115
I. Experimental Investigation under Dry Conditions	116
Results	116
Analytical Data	128
Summary of the Most Significant Results	129
Interpretation of Results	130
Calculation of Fractionation Trends	133
II. Experimental Investigation under Wet Conditions	142
Results	142
Analytical Data	143
Summary of the Most Significant Results	143
Interpretation of Results	145
Calculation of Fractionation Trends	149
Comparison of Experimental Fractionation Trends with Natural Calc-Alkaline Trends	153
Geological Evidence	154
a) Garnet Phenocrysts in Calc-Alkaline Rocks	154
b) Resorbed Quartz Phenocrysts in Calc-Alkaline Rocks	155
c) Trace Element Distribution and Isotope Ratios	155
Summary	157
References	159

Introduction

The calc-alkaline suite is comprised dominantly of the basalt-andesite-dacite-rhyolite volcanic series together with their plutonic equivalents, gabbro, diorite, granodiorite and granite. Representatives of this suite, particularly intermediate and acidic types, are the most abundant igneous rocks in orogenic belts. The association of this rock suite with past and present tectonically active zones is suggestive of a close relationship between the genesis of calc-alkaline rocks, the fundamental mechanism of orogenesis and the evolution of continental areas (WILSON, 1954; ENGEL, 1963). RUBEY (1951, 1955) has argued strongly that the earth's atmosphere, hydrosphere and crust have been formed gradually, over geological time, by degassing and fractional melting of the upper mantle. Some mechanism for the derivation of the calc-alkaline series from the upper mantle would provide the most effective means for the formation of the sialic crust, in harmony with the observed abundances and location of the common igneous rock types. Accordingly in this paper the problem of the genesis of the calc-alkaline suite is considered with particular reference to its possible ultimate origin in the upper mantle. A brief description of the salient features of the calc-alkaline series will be given, followed by a review of the various hypotheses of origin of these rocks. Two additional complementary hypotheses of origin will then be outlined and finally high pressure experimental work conducted to test these hypotheses will be described.

Chemistry of the Calc-Alkaline Suite

The characteristic features of the chemistry of the calc-alkaline suite are brought out in a triangular plot of total iron (as FeO), magnesia and alkali contents (soda and potash) of the rocks (the FMA diagram of POLDERVAART, 1949). An example of such a diagram is given and described in a later section, but the main feature is that the rocks of the calc-alkaline suite fall in an almost straight band extend-

ing from the Fe-Mg side to the alkali apex (Fig. 13 and TILLEY, 1950). There is a little iron enrichment relative to magnesium with increasing total alkali content (i.e. with increasing silica content). This contrasts with the typical tholeiitic fractionation trend which shows marked iron enrichment in the early and middle stages of fractionation (e.g. WAGER, 1960; CARMICHAEL, 1964). The calc-alkaline band is most pronounced for compositions ranging from basaltic andesite to rhyolite. The more basic compositions scatter from a distinct band and indicate some iron enrichment relative to magnesia (see Fig. 13). Some of the scatter of these points may also be due to analyses of rocks which are in part accumulative, and do not represent a true liquid line of descent. Although there is little variation in the Mg/Fe ratio of a calc-alkaline sequence as a whole, there is evidence for iron enrichment in individual lava flows as crystallization proceeds under surface or near surface conditions (WILLIAMS, 1932).

The calc-alkaline rock suite is often characterized by high-alumina content ($\sim 17\%$ Al_2O_3) in basaltic to andesitic members. There may be considerable variations in the alkali/lime index between different provinces. In particular lime is high in the Marianas and Japanese provinces and potash is generally low (SCHMIDT, 1957; KUNO, 1950) compared with the Western North American province where potash is generally high and where there are two distinct zones of differing lime contents — a western zone of more calcic volcanic rocks contrasted with an eastern zone of less calcic rocks (WILLIAMS, 1932, 1935; THAYER, 1937; COOMBS, 1939).

It is important to note that chemical analyses of the groundmass of calc-alkaline rocks or groundmass compositions calculated from known bulk compositions and known phenocryst mineralogy and composition, demonstrate that liquids from basaltic andesite to rhyolite in composition exist in some calc-alkaline provinces. Thus WILLIAMS (1934) showed that the glassy groundmass of a hypersthene andesite approached rhyolite in composition, while WILCOX (1954) indicated that the groundmass composition of the Paricutin lavas varied from basaltic andesite to andesite. This is approximately similar to the variation observed in the bulk rock compositions. Similarly KUNO (1950) demonstrated that the groundmass compositions of representatives of the calc-alkaline rocks of Japan varied from basaltic andesite to rhyodacite in composition. This evidence is critical in explaining the origin of this type of calc-alkaline sequence, since any hypothesis of origin must allow the derivation of such a range of liquid compositions (basic to acid) of appropriate chemistry.

In contrast to the evidence for a line of liquid descent in some localities, it has also been demonstrated that some members of the calc-alkaline suite have been derived by hybridization of an acid magma by basic igneous rocks e.g. WILKINSON (1966) and WILKINSON *et al.* (1964) describe and discuss the formation of an adamellite porphyrite by such a mechanism, thus illustrating a case where no continuous line of liquid descent occurs.

Mineralogy of the Calc-Alkaline Suite

The mineralogy and petrography of the calc-alkaline series are characterised by non-equilibrium assemblages and markedly porphyritic texture. The members

of the series display large phenocrysts with varying degrees of zonation and resorption set in a glassy or fine grained groundmass. In the more basic members (basalts to some andesites) the groundmass is usually crystalline, while in the acid members (dacites to rhyolites) it is usually glassy.

The phenocryst minerals include mainly plagioclase, clinopyroxene, orthopyroxene, hornblende and quartz, with occasional biotite, opaque minerals, olivine and garnet. In the glassy acid representatives of the calc-alkaline suite quartz and plagioclase are the most common phenocrysts, often showing signs of resorption. Biotite and almandine-rich garnet occur rarely. In the more basic compositions (basaltic andesite, andesite), plagioclase is by far the most abundant phenocryst and groundmass mineral comprising 50—70% of the rock. Phenocrysts are typically zoned, with either normal, oscillatory or reversed zones, often with resorbed margins to some of the zones. The zoning may range from bytownite to oligoclase.

Phenocrysts of both hypersthene and augite are common. They sometimes show evidence of resorption (e.g. SCHMIDT, 1957). Hypersthene is the most common groundmass ferromagnesian mineral (TAYLOR and WHITE, 1965) but clinopyroxene has also been recorded (VERHOOGEN, 1937; COOMBS, 1939). Hornblende is the characteristic ferromagnesian phenocryst in some provinces e.g. Japan and the Aleutians but is relatively uncommon in the Marianas Islands, New Zealand and western North America. It usually shows marked resorption. Minor olivine phenocrysts occur in some basaltic andesites and less frequently in andesites where they are usually surrounded by hypersthene coronas (COATS, 1952; COOMBS, 1939; WILCOX, 1954; WILLIAMS, 1932, 1934). Opaque mineral phenocrysts (magnetite or ilmenite) are not common and if they occur comprise < 5% of the rock. Minute opaque crystals are sometimes scattered through the glassy groundmass, reflecting late-stage sub-aerial oxidation of the rocks during eruption.

Hypotheses of Origin of the Calc-Alkaline Igneous Rock Suite

The calc-alkaline suite consists of a complex association of rock types exhibiting a complex history of crystallization. These features have made it difficult for petrologists to interpret the origin of these rocks, and accordingly several different hypotheses of origin have arisen. There is convincing evidence for a polygenetic origin of the calc-alkaline suite, and it is improbable that a single hypothesis of origin will satisfy all the features of the suite from different localities.

a) Fractional Crystallization of Basaltic Magma

BOWEN (1928) considered that the calc-alkaline rock series was derived by simple fractional crystallization of a basaltic magma. However this is not an efficient mechanism for enrichment in silica because of the moderate silica content of the crystal extract (low-alumina pyroxene, olivine and plagioclase). Thus an initially immense volume of basalt would be required to produce the large volumes of intermediate to acid calc-alkaline compositions observed, and basalt is often not an abundant member of the calc-alkaline series. Also the end product of the fractional crystallization of a tholeiitic basalt magma is tholeiitic andesite (icelandite)

or iron-rich granophyre, rather than an orogenic andesite, dacite or rhyolite. The fractionation trends as depicted on an FMA plot for the crystallization of a typical tholeiitic basalt and for the calc-alkaline series are quite different, indicating different mechanisms of origin. POLDERVAART and ELSTON (1954) list several specific limitations to BOWEN's hypothesis.

OSBORN (1959, 1962), on the basis of experimental studies on simple iron-bearing silicate systems under controlled oxidation conditions, suggested that the calc-alkaline rock suite may be derived by fractional crystallization of a basaltic magma under constant oxygen pressures, possibly achieved by high water vapour pressures. He claimed that under such conditions magnetite crystallised out early, relative to plagioclase. This prevented iron-enrichment and promoted silica-enrichment. However this mechanism does not generally satisfy the chemical and petrographic features of the rocks of the calc-alkaline series. For example, calc-alkaline rocks are not invariably significantly oxidized (Table 1), and many of the cases of marked oxidation may be attributed to late stage processes, such as sub-aerial oxidation during eruption. Also there is a general lack of evidence

Table 1. *Oxidation state of calc-alkaline rocks*

Note: Only a few selected analyses of calc-alkaline rocks are given; this is not intended as an exhaustive survey. The original oxidation state of the magma is likely to be lower than the figures listed because of the effects of high-level or sub-aerial oxidation of the analysed rocks.

Rock type	FeO	Fe ₂ O ₃	FeO/Fe ₂ O ₃	Reference
Basalt	6.69	1.51	4.4	WILLIAMS (1942)
	8.59	2.21	3.9	WILLIAMS (1933)
	6.41	1.24	5.2	WILLIAMS (1950)
Basaltic andesite	4.98	1.47	3.4	WILLIAMS (1942)
	5.07	1.91	2.7	WILLIAMS (1950)
	7.8	1.7	4.6	BYERS (1961)
Andesite	4.21	1.59	2.6	WILLIAMS (1942)
	4.00	0.97	4.1	WILLIAMS (1950)
	7.38	1.01	7.3	WILLIAMS (1935)
	5.93	2.23	2.7	SCHMIDT (1957)
	4.66	1.10	4.2	WILCOX (1954)
Dacite	2.56	0.37	6.9	WILLIAMS (1942)
	1.12	0.29	3.9	SCHMIDT (1957)
	3.61	1.12	3.2	COOMBS (1939)
Rhyolite	1.76	0.24	7.3	WILLIAMS (1935)
	1.53	0.88	1.7	WILLIAMS (1932)

for early crystallization of magnetite; instead there is abundant evidence for early crystallization of plagioclase, which greatly reduces the efficiency of OSBORN's model, particularly in the basalt to andesite part of the calc-alkaline series. The intermediate-acid members of the calc-alkaline series do not show marked depletion in Ti or V as would be expected (WAGER and MITCHELL, 1951) if an opaque mineral (e.g. titanomagnetite) was a key phase in the formation of such compositions (TAYLOR and WHITE, 1966; COATS, 1952, 1959; SNYDER, 1959; BYERS, 1961; DREWES *et al.*, 1961). There is little or no field evidence for an association of

opaque mineral-rich mafic crystalline residua with the development of the calc-alkaline series. Some of the Alaskan zoned ultramafic complexes have the appropriate composition, but it has been argued that these complexes formed from ultramafic magmas and in most cases show no evidence for residual crystal accumulation from a basaltic parent (RUCKMICK and NOBLE, 1959; TAYLOR and NOBLE, 1960; exceptions are described by IRVINE, 1963).

Recent work by CARMICHAEL (1967) on iron-titanium oxides occurring in some acid calc-alkaline rocks indicates that oxygen fugacity has not remained constant during fractionation in the volcanic series, as required by OSBORN's model. Also WILKINSON (1966) pointed out that titanomagnetites described from Japanese andesites (AKIMOTO, 1954, 1955) implied crystallization under conditions of low oxygen pressure. In other areas hornblendes and biotites in more acid members of the series show considerable iron-enrichment, not expected according to OSBORN's hypothesis (LARSEN and DRAISIN, 1950).

b) Melting of Pre-Existing Sial, Hybridism or Mixing of Magmas

Partial or complete melting of deep crustal sialic material of appropriate composition has been considered as a possible origin for the various members of the calc-alkaline series (HOLMES, 1932; HESS, 1960; TURNER and VERHOOGEN, 1960). When partial melting takes place magmas of rhyolitic composition may be produced first, followed progressively by dacite, andesite and finally basaltic andesite as the temperature of the partial melting increases.

Alternatively hybridization of the early formed acid magma may occur, producing more basic members of the calc-alkaline suite. Thus NOCKOLDS (1934) proposed that diorite, tonalite and granodiorite plutonic members of the calc-alkalite suite were derived from the interaction of acid quartzo-feldspathic magma with solid basic igneous material. WILKINSON (1966) elaborated on this mechanism, proposing hybridization of an acid magma by dioritic rocks, and WILKINSON *et al.* (1964) described an adamellite-porphyrite from New England which demonstrated hybridization of a low melting silicic alkalic liquid by a biotite diorite.

Mixing of acid and basic magmas has been suggested as a means of deriving magmas of intermediate composition. The basic magma is derived from the mantle while the acid magma comes from melting of sialic crustal material. Mixing of magmas has been demonstrated in some instances (LARSEN *et al.*, 1936; WILLIAMS *et al.*, 1955; MACDONALD and KATSURA, 1965).

All these theories involving development of magma from sialic material fail to explain the origin of calc-alkaline rocks occurring along the borders of some ocean basin regions where there is no sialic material available e.g. calc-alkaline rocks in island arc regions developed across oceanic crust as in the Kuriles (KOSMINSKAYA, 1963), Aleutians (SHOR, 1964) and the Marianas Islands (GORSHKOV, 1962). Similarly these theories cannot account for the evolution of sialic continents from the earth's mantle as implied in the hypotheses of RUBEY (1955), WILSON (1954) and ENGEL (1963). In addition some geochemical data on the calc-alkaline suite precludes large scale involvement of sialic material in its genesis. Thus low initial strontium isotope ratios found for calc-alkaline rocks from many localities (TAYLOR and WHITE, 1965; HURLEY *et al.*, 1965 and EWART and STIPP, 1967) indicate that

they cannot have formed from pre-existing old crustal material enriched in radiogenic strontium. Similarly the observed trace element and rare earth element abundances in andesite preclude large scale contributions from sialic material e.g. low content of K, Rb, U, Th, rare earths, Sn and Li in andesites (TAYLOR and WHITE, 1966). It is significant that recent work has shown that the calc-alkaline series of oceanic island arc regions is chemically distinct from the calc-alkaline series of continental areas e.g. the series in island arc regions is lower in K than the series in continental areas (DICKINSON, 1967). This type of difference may be linked with different origins of the calc-alkaline rocks of these regions. The hybridization and mixing of magma theories, though demonstrated in some particular cases, fail to explain the evidence for a liquid line of descent in the calc-alkaline series in other areas. Liquids of composition ranging at least from basaltic andesite to rhyolite occur (see p. 107).

c) Contamination of Basaltic Magma with Sialic Crust

DALY (1933) suggested that sialic material incorporated into basaltic magma gave rise to most andesites. Similarly TILLEY (1950) proposed that the calc-alkaline series was derived from fractional crystallization of basaltic magma modified by sialic contamination. This hypothesis has also been followed by KUNO (1950), WATERS (1955) and WILCOX (1954). However this hypothesis, although possibly applicable in some localities, fails as a general explanation for the origin of the calc-alkaline series; in particular it cannot explain the development of the calc-alkaline series in island arcs which have formed across oceanic crust, where no sial occurs.

d) Partial Melting of Quartz Eclogite at 100—150 kms Depth

O'HARA (1963) demonstrated that under dry conditions at a pressure of 30 kb the garnet-pyroxene tie line forms a thermal barrier between undersaturated olivine- and oversaturated quartz-bearing assemblages. Thus oversaturated magmas may only be derived at great depth in the mantle if parent oversaturated compositions (e.g. quartz eclogite) are present in the mantle, and undergo partial melting. However several lines of evidence indicate that the mantle has an undersaturated composition, probably approximating to 3 parts peridotite and 1 part basalt (termed pyrolite; RINGWOOD, 1966). Hence the derivation of the oversaturated calc-alkaline series is not possible by the simple partial melting of the pyrolite mantle at depth.

Recently RINGWOOD and D. H. GREEN (1966), after a study of the gabbro-eclogite transformation, proposed a new model for orogenic processes which provides a mechanism for obtaining oversaturated quartz eclogite compositions in the upper mantle. According to this model, it is envisaged that in present or possible future active orogenic regions of the earth's crust such as island arcs, some oceanic rises, oceanic rift systems and continental margins, large piles of basalt have developed as the first stage in the cycle of orogenic activity and continental growth. As long as active basaltic volcanic activity persists, the geotherms in the particular region remain high. However, with cessation of volcanic activity the geotherms fall and the deeper regions of the basaltic pile begin to

transform to eclogite¹. The quartz eclogite ($\rho \sim 3.45 \text{ gm/cm}^3$) is denser than the ultramafic upper mantle ($\rho \sim 3.3 \text{ gm/cm}^3$) so that it begins to sink into the mantle. In the early stages, sinking is relatively slow, and results in formation of a geosyncline. At a later stage, sinking becomes catastrophic, leading to severe crustal deformation and folding of the geosyncline. Eventually, the sinking eclogite bodies reach a level in the mantle (probably at depths of 100–150 km) where the temperature is sufficiently high to cause partial melting of the eclogite. Magmas thus produced rise upwards and intrude the folded geosyncline. The possibility is suggested that these magmas may represent the calc-alkaline suite.

This hypothesis formed the basis of one of the series of experiments described in this paper. These experiments have aimed at determining whether rocks of typical saturated or near-saturated basaltic composition, when subjected to fractional melting and fractional crystallization at pressures of 30 to 40 kb, are capable of yielding large proportions of typical calc-alkaline magmas, e.g. andesites and granodiorites. Preliminary results, favourable to this hypothesis, have been outlined in a previous paper (T. H. GREEN and RINGWOOD, 1966).

e) Partial Melting of Basalt at 30–40 kms Depth under Wet Conditions
($P_{\text{H}_2\text{O}} < P_{\text{LOAD}}$)

DALY (1933), HAMILTON (1964), COATS (1962), LIDIAK (1965), BRANCH (1967) and others have suggested that the calc-alkaline series may be generated by "wet" partial melting or crystallization of mafic material near the base of the crust or in the upper mantle. Although this hypothesis has been the subject of a considerable amount of speculative discussion, direct supporting evidence, particularly of an experimental nature, is practically non-existent. In the present paper, we propose to develop this hypothesis further, and to subject it to a quantitative experimental investigation.

As in the previous model (d), it is envisaged that in the first stage large piles of basalts develop in the earth's crust in such areas as island arcs, some oceanic rises, oceanic rift systems and continental margins. In this case limited access of water to the basalt pile takes place, due possibly to the repeated extrusion of comparatively thin submarine lava flows. As the pile grows the basalt in the deeper regions where the temperature may be of the order of 400° C will alter to amphibolite.

Subsequently a higher temperature distribution may be obtained in the amphibolite, either as it is buried still further due to continuing volcanic activity, or at a later stage after a period of quiescence followed by a renewed phase of volcanic activity. Under these high temperature conditions partial melting of the amphibolite may take place. In the present study we shall investigate the possibility that this melting may produce magmas of the calc-alkaline suite, leaving a

¹ There is an extensive range of olivine-normative basaltic compositions which, together with quartz-normative basalts, will transform to quartz-bearing eclogites under appropriate conditions (e.g. high-alumina olivine tholeiite with 9.3% normative olivine has 8.5% normative quartz when calculated in terms of an eclogite norm — RINGWOOD and D. H. GREEN, 1966). Most basalts occurring in large scale basaltic volcanic provinces, e.g. Hawaii (MACDONALD and KATSURA, 1964) and Iceland (CARMICHAEL, 1964) are olivine or quartz-normative tholeiites and fall into the category producing quartz-bearing eclogites, if they transform to an eclogite assemblage.

residuum of amphibole, pyroxenes and possibly minor calcic plagioclase and garnet. According to the model, the residuum may remain as a basic amphibole-rich lower crust with a V_p of about 7.5 km/sec, overlain by a sialic upper crust consisting of the calc-alkaline rocks extracted from the parental amphibolite. The upper crust has a much lower seismic velocity in the vicinity of 6 km/sec. Alternatively if most of the water is driven from the residual amphibolite while high temperature conditions prevail, then the amphibolite would change to a granulite assemblage. Then, when volcanic activity has ceased and the abnormally high temperature-depth distribution had returned to normal, the granulite may over a long period of time transform to eclogite. The residuum from the partial melting will be comparatively poor in alkalis and similar to a nepheline basanite. The work of D. H. GREEN and RINGWOOD (1967a) demonstrates that such a composition would transform to eclogite at a lower pressure than other basalts. If the transformation to eclogite takes place then the residuum may subsequently sink into the mantle (cf. RINGWOOD and D. H. GREEN, 1966).

A second series of experiments to be described in this paper was designed to investigate this hypothesis. In these experiments the fractional melting and fractional crystallization of a saturated basalt have been studied at 9–10 kb. at conditions of $P_{H_2O} < P_{LOAD}$.

The hypotheses (d) and (e) are essentially complementary to each other since they both involve derivation of the calc-alkaline suite by a two-stage magmatic process, incorporating in the first stage large scale extrusion of saturated basaltic magma in the earth's crust. The subsequent history of this basalt pile, whether it remains dry and transforms to eclogite, or whether water has access while high temperature conditions pertain, determines whether the calc-alkaline suite is produced according to model (d) or (e). Both models might explain the derivation of the suite in areas where no sialic material occurs and also provide a mechanism for continental evolution from an undersaturated upper mantle.

Since minor basalt magma is frequently erupted along with the more abundant calc-alkaline magmas (basaltic andesite — andesite — rhyolite), the two complementary hypotheses (d) and (e) for the origin of the calc-alkaline series, must also explain this close association with basalt magma. In the case of the first hypothesis (d), the calc-alkaline magmas rising from the partial melting of quartz eclogite at 100–150 kms depth may cause instability in the mantle at shallower levels. This may result in renewed fractional melting in the upper mantle giving basalt magmas as discussed in detail by D. H. GREEN and RINGWOOD (1967b) and T. H. GREEN, D. H. GREEN and RINGWOOD (1967). This second generation of basalts may then rise to the surface in association with the liquids obtained by partial melting of the quartz eclogite. Alternatively in the case of the second hypothesis (e), a high temperature gradient is needed in the amphibolite to allow partial melting. Renewed or continued basaltic volcanism from the mantle is the most likely ultimate cause of this high temperature gradient, so that the association of basalt lavas with calc-alkaline lavas at the earth's surface is to be expected.

Thus in both these models the occurrence of basalts with the calc-alkaline series may be explained as a function of the thermal mechanism giving rise to the series, rather than as a direct chemical link between the basalts and the more sialic rocks of the calc-alkaline suite.

Linked with these two models there is a third possible way in which the calc-alkaline series may be derived. In this third model a basaltic magma is contaminated with water and undergoes fractional crystallization under hydrous conditions (with $P_{H_2O} < P_{LOAD}$) at 30–40 kms depth. The crystallization will be dominated by amphibole, and to a smaller extent will involve pyroxenes, and possibly calcic plagioclase and garnet. The residual liquids derived from this crystallization will correspond to intermediate or acid members of the calc-alkaline suite, depending on the degree of fractional crystallization. Circumstances where water may have access to a basalt magma at 30–40 kms depth could occur at the margins of the oceans, where, according to the hypothesis of sea-floor spreading (HESS, 1962) downward “convection currents” are present. These “currents” may carry hydrated rocks into contact with basalt magma derived by partial melting of the mantle (cf. D. H. GREEN and RINGWOOD, 1967b). The sea-floor spreading hypothesis may also be linked to the sinking eclogite model for the origin of calc-alkaline rocks (RINGWOOD and D. H. GREEN, 1966).

Experimental

The experimental procedure followed has been to prepare a series of glasses with compositions approximating to typical members of the calc-alkaline series, high-alumina olivine tholeiite, high-alumina quartz tholeiite, basaltic andesite, andesite, dacite and rhyodacite. After fusion, the oxidation state and iron content have been checked by chemical analysis (E. KISS, A. J. EASTON, A.N.U. analysts), and in some cases the glass composition has been further checked by electron microprobe analysis. The compositions are listed in Table 2. The basalts chosen are high-alumina tholeiitic types similar to basalts found associated with the calc-alkaline series e.g. western North America (ANDERSON, 1941; WILLIAMS, 1935 and THAYER, 1937), Japan (KUNO, 1960) and New Zealand (CLARK, 1960) and similar to basalts dredged from ridges of the Atlantic, Pacific and Indian Oceans (ENGEL, ENGEL and HAVENS, 1965; ENGEL, FISHER and ENGEL, 1965). Apart from the high-alumina content, the quartz tholeiite is approximately similar to the overall composition of many major basalt sequences e.g. continental flood basalts (TURNER and VERHOOGEN, 1960) and basalt piles in oceanic areas (Hawaii: MACDONALD and KATSURA, 1964; Iceland: CARMICHAEL, 1964).

The andesite composition (Table 2) was originally prepared for a different problem (T. H. GREEN, 1967a, b) and compared with the dacite chosen for this investigation it has a slightly high potash content. Initially, as an approximation to a rhyodacite composition an adamellite (termed rhyodacite I in this paper) previously prepared and described by D. H. GREEN and LAMBERT (1965) was used.

The glasses have been subjected to a wide range of closely controlled temperature-pressure conditions in a piston-cylinder, high pressure and high temperature apparatus similar to that described by BOYD and ENGLAND (1960, 1963). The high pressure experimental techniques involved have been described fully elsewhere (D. H. GREEN and RINGWOOD, 1967a). A pressure correction of –10% has been applied and the resulting pressures are believed to be accurate to $\pm 3\%$ in the range 15–40 kb (T. H. GREEN, RINGWOOD and MAJOR, 1966).

A detailed study of fractional crystallization and crystal-liquid equilibria in the different compositions listed in Table 2 has been made at a series of pressures up to 36 kb. The nature, proportion and composition of mineral phases present have been determined by optical, x-ray and electron microprobe techniques, and the principal fractionation trends at high pressure have been established. In this way the model for the origin of the calc-alkaline series by fractional melting of quartz eclogite at 100–150 kms has been tested experimentally. In addition to this detailed dry high pressure study, a series of reconnaissance runs have been carried out under wet conditions. The procedure followed has been use to undried pressure cell components without boron nitride sleeves. The sample is packed into a thin walled platinum tube and about 1 mgm of water added. The tube is then crimped, but not sealed. Wet runs have generally been conducted for 1–8 hours. This procedure results in uncontrolled

Table 2. Compositions and norms of rock mixes used in the experimental work

	1. High- alumina olivine tholeiite	2. High- alumina quartz tholeiite	3. Basaltic andesite	4. Andesite	5. Dacite	6. Rhyodacite I (adamellite)
SiO ₂	50.3 ^a	52.9	56.4	62.2 ^a	65.0 ^a	69.6
TiO ₂	1.7 ^a	1.5	1.4	1.1 ^a	0.7 ^a	0.6
Al ₂ O ₃	17.0 ^a	16.9	16.6	17.3 ^a	16.1 ^a	14.7
Fe ₂ O ₃	1.5 ^b	0.3 ^b	3.0 ^b	0.3 ^b	1.4 ^b	1.7 ^b
FeO	7.6 ^b	7.9 ^b	5.7 ^b	5.9 ^b	3.5 ^b	1.8 ^b
MnO	0.16	0.2	0.1	0.1	0.1	0.1
MgO	7.8 ^a	7.0	4.3	2.4 ^a	1.8 ^a	1.0
CaO	11.4 ^a	10.0	8.5	5.2 ^a	5.0 ^a	2.5
Na ₂ O	2.8 ^a	2.7	3.0	3.3 ^a	3.6 ^a	3.4
K ₂ O	0.18 ^a	0.6	1.0	2.3 ^a	2.1 ^a	4.6
	100.4	100.0	100.0	100.1	99.3	100.0
MOL. PROP. 100 MgO	60.7	60.4	47.7	41.0	40.3	36.0
<hr/>						
MgO + FeO _{Total}						
CIPW NORMS						
Qz	—	1.3	10.7	15.5	21.7	25.3
Or	1.1	3.5	5.9	13.6	13.0	27.2
Ab	23.7	22.8	25.4	27.9	30.5	28.8
An	33.3	32.2	28.9	25.7	21.5	11.2
Diop	18.9	14.2	10.8	0.2	2.3	0.9
Hyp	11.9	22.6	11.3	14.8	7.7	3.0
Ol	6.2	—	—	—	—	—
Mt	2.2	0.4	4.3	0.4	2.0	2.5
Ilm	3.2	2.8	2.7	2.1	1.3	1.1

^a Denotes content determined by electron probe analysis of a glass fragment.

^b Denotes chemically determined content (E. Kiss, A. N. U., analyst).

wet conditions during the experiment, with P_{H_2O} undoubtedly less than P_{LOAD} . With practice consistent and reproducible results could be obtained following this method. Wet runs were carried out on high-alumina quartz tholeiite, basaltic andesite and andesite compositions in order to experimentally test the model suggesting that the calc-alkaline series may be derived by fractional melting of basalt under conditions of $P_{H_2O} < P_{LOAD}$ at 30–40 kms depth. The experimental method is not ideal because of some iron loss in the long experiments, and the uncertainty of the P_{H_2O} on the sample, but with the type of apparatus used this method was the best that could be achieved.

Analytical

The analytical procedures followed involved electron microprobe determination of the compositions of clinopyroxene, orthopyroxene, garnet, plagioclase and amphibole crystals in polished sections of the products of the high pressure experimental runs. Direct calibration has been carried out between the phases analyzed and prepared standard synthetic orthopyroxene, "clinopyroxene" and "feldspar" glasses and natural, analyzed garnet standards of overall similar composition to the experimental crystal phases. Because of this similarity in composition no correction procedures have been followed, and the method of counting for fixed specimen currents has been adopted. Using these methods accuracy of analysis is estimated to be of the order of 5% of the amount present for analyses of SiO₂, TiO₂, Al₂O₃, FeO, MgO, MnO, CaO and K₂O and about 10% for Na₂O. Thus when the analyses for these major elements are totalled, figures in the range from 95–105% are considered to be reason-

able. This is sufficiently accurate for the purpose of indicating fractionation trends of the major elements in certain magmas at high pressure, the main aim of this experimental project.

However if the analyzed phases total outside a range of, for example 99–101% and these unchanged analyses are used to calculate derivative liquids by extracting estimated amounts of crystals of these compositions from the starting composition, then the totals for the residual liquids or crystal aggregates will be correspondingly poor, and may be misleading (e.g. in calculation of normative compositions). These totals should not arbitrarily be corrected back to 100% because the errors in the original analyses may not have been proportionately distributed between the components. If the probe analyses total outside the range 99–101% or where the calculated liquid fractionate compositions fall outside this range, the procedure adopted to reduce these discrepancies is as follows: The electron microprobe analyses obtained are used as the basis for the calculation of the composition of the phase so that this totals 100% and fits the stoichiometry of the phase concerned. The calculated compositions are then used in the determination of the fractionation trends. In subsequent tables where this has been done the liquid fractionates or crystal residua are marked.

Because fractionation trends involving iron are important in the calc-alkali series, iron losses from the samples to the platinum capsules during a run may result in errors in the calculation of fractionation trends. Chemical analysis for ferrous and ferric iron in some of the higher temperature (above liquidus) runs has been carried out (E. Kiss, A.N.U. analyst) in order to place approximate upper limits on the likely iron loss. These analyses are given in Table 3. Also to reduce this iron loss effect, run times above 1300°C have been shortened and also only crystals away from the edge of the sample have been analysed. Iron loss is minimal in the central areas of the samples. As an additional check on the iron loss effects in the experiments conducted under wet conditions in platinum capsules, a few wet runs have been carried out in graphite capsules and the compositions of the phases crystallized in the two different types of capsules have been compared.

Table 3. *Changes in iron content and oxidation state during experimental runs (Analyses by E. Kiss, A. N. U.)*

Composition	Conditions of run			FeO		Fe ₂ O ₃		Total Fe as FeO	
	Temp. (°C)	Pressure (kb)	Time (Hrs)	Initial	Final	Initial	Final	Initial	Final
High-alumina olivine tholeiite	1,360	18	1	7.6	3.5	1.5	0.9	9.0	4.3
	1,440	27	1/2	7.6	4.1	1.5	0.06	9.0	4.15
High-alumina quartz tholeiite	1,360	18	2/3	7.9	4.1	0.3	0.5	8.2	4.6
	880	10	8 (wet)	7.9	5.9	0.3	0.2	8.2	6.1
	1,020	10	4 (wet)	7.9	5.6	0.3	0.1	8.2	5.7
Basaltic andesite	1,400	27	1/2	5.7	6.2	3.0	0.1	8.4	6.3
Dacite	1,320	18	5/6	3.5	2.7	1.4	0.1	4.8	2.8
	1,280	27	5/6 (wet)	3.5	2.2	1.4	0.3	4.8	2.5
	1,220	27	2/3 (wet)	3.5	2.2	1.4	0.1	4.8	2.3

I. Experimental Investigation under Dry Conditions

Results

The results of the phase equilibria in the partial melting fields of the various compositions under dry conditions for the pressure range 18–36 kb are the main concern of this section. The details of the dry experimental runs are recorded in Tables 4–9 and are summarized in Figs. 1–6. In consulting these tables and

Table 4. Results of the experimental runs in the 27–36 kb range on the high-alumina olivine tholeiite composition. Results of runs at 18 kb are given elsewhere (T. H. GREEN, 1968)

Conditions of the run			Phases present	Esti- mated % of glass	R. I. (± 0.01)	Comments and esti- mated relative propor- tions of crystal phases present
Pres- sure (kb)	Temp- erature ($^{\circ}$ C)	Time (mins)				
27	1,360	60	cpx ga q-px glass	?	1.74	Well crystallized, large primary crystals, quench pyroxene common; cpx > ga
27	1,400	40	cpx ga q-px glass	?	1.745	Well crystallized, euhedral garnet and stubby clinopyroxene; cpx > ga
27	1,420	30	cpx ga q-px glass	?	1.74	Well crystallized, (as above); cpx > ga
27	1,430	25	cpx ga q-px glass	?	1.74	Moderately common primary cpx, uncommon garnet; cpx > ga
27	1,435	30	cpx q-px glass	?		Moderate amount of primary cpx, no ga observed
27	1,440	30	glass	100		No crystals evident, above liquidus
36	1,520	15	cpx ga q-px glass	?	1.74	Well crystallized stubby primary cpx and euhedral ga, cpx > ga
36	1,535	10	cpx ga q-px glass	?		Minor euhedral garnet, rare primary clinopyroxene; ga > cpx.

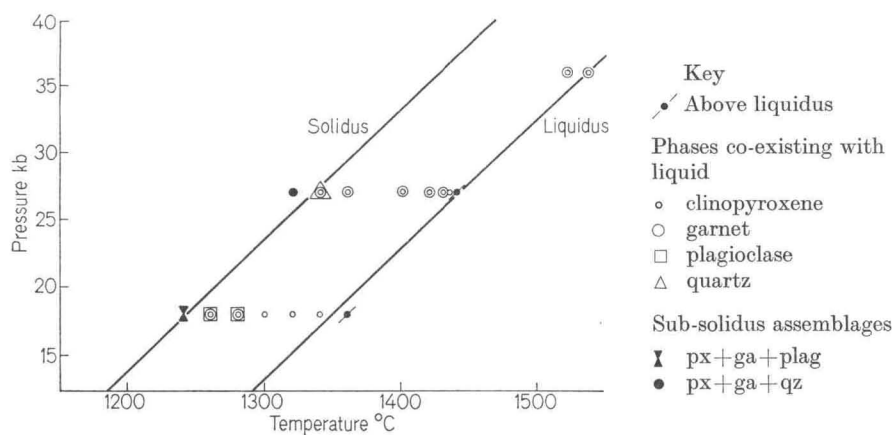


Fig. 1. Results of the experimental runs on the high-alumina olivine tholeiite composition

Experimental runs on the high-alumina quartz tholeiite composition under dry conditions

Phases present	Estimated % of glass	R.I. garnet (± 0.01)	Comments and estimated relative phases present
cpx plag ga qz ? ore			Sub-solidus run, moderate grain size, accessory opaque minerals and very minor quartz.
cpx plag ga glass	35	1.77	Abundant moderate sized pyroxene, large garnet and plagioclase base; $\text{cpx} \gg \text{plag} > \text{ga}$
cpx glass	85		Common clinopyroxene; estimated
cpx glass	99		Rare clinopyroxene, very near liquidus
cpx glass	100		Above-liquidus run.
cpx ga qz	—		Sub-solidus run, fine grained;
cpx ga glass	20	1.765	Moderate grain size; $\text{cpx} \gg \text{ga}$.
cpx ga glass	65	1.755	Well crystallized; $\text{cpx} \gg \text{ga}$.
cpx ga q-px glass	?	1.76	Common clinopyroxene, minor garnet; $\text{cpx} > \text{ga}$.
cpx ga q-px glass	?		Common clinopyroxene, quenched garnet.
cpx q-px glass	?		Rare primary clinopyroxene, very minor garnet.
cpx ga qz ? q-px	?	1.76	Abundant primary clinopyroxene, common garnet (5% approx.) and quartz.
cpx ga q-px glass	?	1.755	Common primary and quenched garnet (10% approx.)
cpx ga q-px glass	?	1.75	Common primary and quenched garnet (5% approx.).
cpx ga q-px glass	?	1.75	Common quenched pyroxene, unquenched clinopyroxene and garnet (3%

Table 6. Results of the experimental runs on the basaltic andesite composition

Conditions of the run			Phases present	Esti- mated % of glass	R.I. garnet (± 0.01)	Comments and estimated relative proportions of crystal phases present.
Pres- sure (kb)	Tempe- rature ($^{\circ}$ C)	Time (mins)				
9	1,200	60	cpx plag	glass	75	Medium grainsize; plag \gg cpx.
9	1,220	60	cpx plag	glass	90	Common plagioclase, rare clinopyroxene, well crystallized; plag \gg cpx.
9	1,240	60		glass	100	Above liquidus run.
18	1,200	60	cpx plag ga qz ore		—	Sub-solidus run, fine grained, estimate cpx > plag \gg qz > ga > ore.
18	1,250	60	cpx plag ga	glass	60	Clinopyroxene crystals small, plagioclase and garnet crystals large; cpx \gg plag \gg ga.
18	1,280	60	cpx	glass	90	Common clinopyroxene; estimate 10% cpx.
18	1,300	50	cpx	glass	95	Minor clinopyroxene, estimate 5% cpx.
27	1,250	60	cpx ga qz		—	Sub-solidus run, fine grained; cpx \gg ga, qz.
27	1,300	55	cpx ga qz		—	1.765 Sub-solidus run, medium grained; cpx \gg ga, qz.
27	1,330	45	cpx ga	glass	60	1.765 Medium grained clinopyroxene and garnet; cpx \gg ga.
27	1,360	40	cpx ga q-px	glass	80	1.765 Well-crystallized, some minute needles of quench pyroxene; cpx > ga.
27	1,380	35	cpx ga	glass	90	1.755 Well-crystallized; cpx > ga.
27	1,390	35	cpx ga	glass	95	Well-crystallized, but uncommon crystals; ga > cpx.
27	1,400	30		glass	100	Above liquidus run.
36	1,380	40	cpx ga qz		—	1.76 Sub-solidus run, medium grained; cpx \gg ga > qz.
36	1,440	20	cpx ga q-px	glass	?	1.755 Abundant primary and quench pyroxene, common garnet (15% approx.)
36	1,460	20	cpx ga q-px	glass	?	1.75 Abundant primary and quench pyroxene, common garnet (12% approx.).
36	1,475	15	cpx ga q-px	glass	?	1.75 Rare primary clinopyroxene (difficult to identify because of abundant quench-pyroxene), common garnet (6% approx.).

Table 7. Results of the experimental runs on the andesite (quartz diorite) composition

Conditions of the run				Phases present	Estimated % of glass	R.I. garnet (± 0.01)	Comments and estimated relative proportions of crystal phases present
Pressure (kb)	Temperature ($^{\circ}$ C)	Time (mins)	Dry or Wet ^a (D or W)				
18	1,000	240	W	cpx plag ga qz	—		Sub-solidus run, fine grained except for medium sized garnet crystals; plag > qz > cpx \gg ga.
18	1,220	60	D	cpx plag ga qz glass	60		Medium grained; plag \gg cpx > qz > ga.
18	1,260	60	D	plag ga glass	85		Common well crystallized plagioclase, rare large garnets; plag \gg ga.
18	1,275	60	D		100		Above-liquidus run.
22.5	1,000	240	D	cpx plag ga qz	—		Sub-solidus run, fine grained; qz > cpx > pl \gg ga.
22.5	1,300	60	D	cpx ga glass	95	1.77	Well-crystallized; ga > cpx.
27	1,000	240	W	cpx felds ga qz	—		Sub-solidus run, fine grained except for medium sized garnet crystals; qz, cpx \gg ga > felds.
27	1,000	240	D	cpx felds ga qz			Indistinguishable from above wet run at same P—T conditions.
27	1,150	60	D	cpx felds ga qz			Fine grained pyroxene and low R.I. phase; medium grained garnet; qz, cpx > ga > felds.
27	1,240	60	D	cpx plag ga qz	—		Probable near-solidus run, medium grainsize; qz, plag > cpx, ga.
27	1,280	60	D	cpx plag ga qz glass	20		Medium grainsize, similar to above run except qz, plag proportion slightly smaller relative to cpx, ga but qz, plag > cpx, ga in this run also.
27	1,320	60	D	cpx ga qz glass	60	1.765	Well crystallized; cpx \gg ga \gg qz.
27	1,340	60	D	ga glass	95	1.765	Uncommon, very well crystallized garnet.
31.5	1,000	240	W	cpx felds ga qz			Sub-solidus run, fine grained except for medium grained garnet; qz > cpx > ga \gg felds
36	1,340	30	D	cpx felds ga qz ?glass	?		Uncertain solidus run, may be very minor melting, medium grained; qz > cpx > ga \gg felds.
36	1,400	30	D	cpx ga qz glass	40	1.765	Well crystallized; cpx \gg ga \gg qz.
36	1,420	20	D	cpx ga glass	90	1.765	Large garnet crystals, small pyroxene crystals; ga \gg cpx.
36	1,440	15	D	ga glass	95	1.76	Large garnet crystals, uncommon.

^a In these wet runs no water added to mix, dried pyrophyllite spacer used.

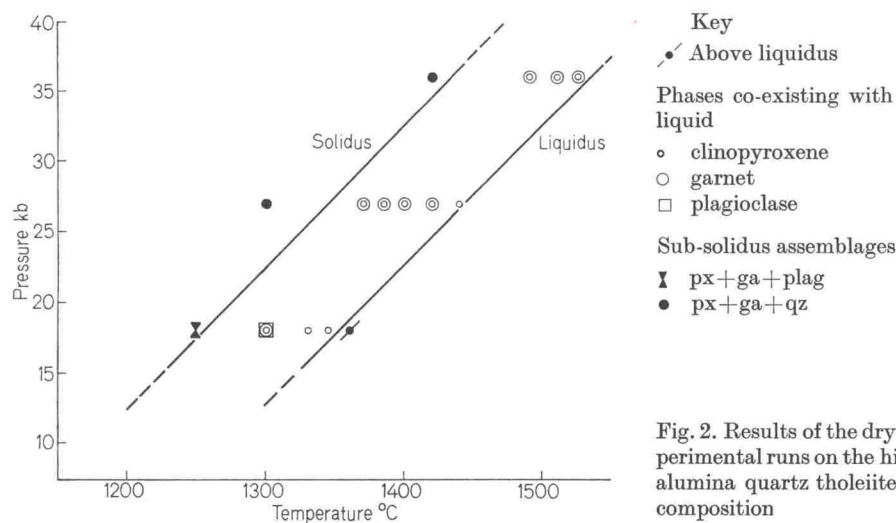


Fig. 2. Results of the dry experimental runs on the high-alumina quartz tholeiite composition

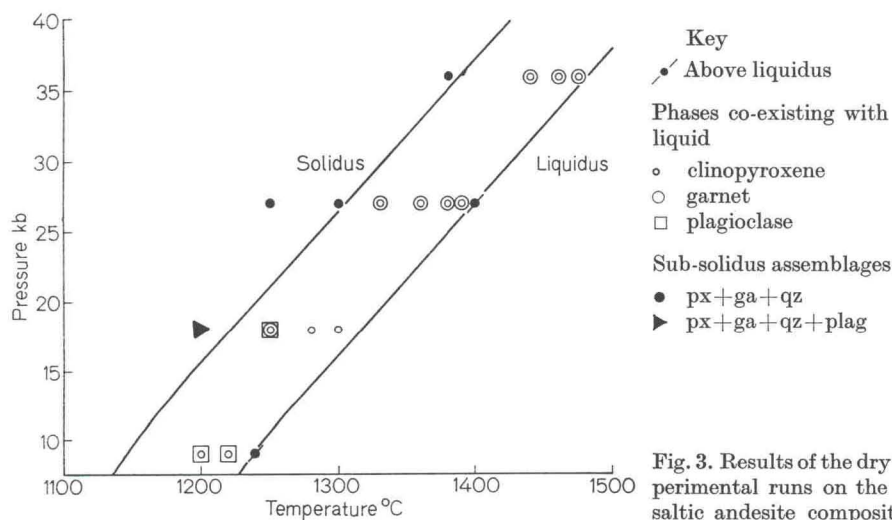


Fig. 3. Results of the dry experimental runs on the basaltic andesite composition

diagrams it should be pointed out that estimates of degree of crystallization and determination of the solidus temperature are hampered in both the basaltic compositions at 27–36 kb and also in the basaltic andesite composition at 36 kb, because of the presence of quench-pyroxene. However, with care, the primary and quench-pyroxenes can be distinguished optically. A brief description of the characteristic features of the petrography of the runs is given as follows.

Plagioclase is distinguished as small to medium sized (50 μ long) acicular crystals sometimes showing multiple twinning in runs near the liquidus. In near-solidus runs plagioclase crystals are difficult to distinguish from amoeboid glass but may be identified by X-ray means. Primary clinopyroxene occurs as medium sized

Experimental runs on the dacite composition under dry conditions

Phases present	Estimated % of glass	Comments and estimated relative proportions of
cpx plag qz ?glass	> ?	Uncertain solidus run, fine grained; plag > qz ≫
cpx plag qz ? glass	60	Medium grainsize, uncertain presence of quartz
plag glass	75	Medium grainsize, estimate 25% plagioclase.
plag glass	90	Medium grainsize, estimate 10% plagioclase.
plag glass	> 99	Very rare plagioclase laths, near-liquidus run.
cpx plag ga qz glass	30	Medium grainsize; plag > qz > cpx > ga.
cpx plag ga qz glass	50	Medium grainsize; plag, qz ≫ cpx > ga.
cpx plag qz glass	65	Medium grainsize; plag, qz ≫ cpx.
plag qz glass	80	Medium grainsize; approx. equal proportions of
plag qz glass	> 95	Minor small quartz crystals.
plag qz glass	100	Above-liquidus run.
cpx felds qz —	—	Very fine grained; qz, cpx ≫ felds; no garnet id
cpx felds ga qz glass	20	Fine grained except for large, inclusion-filled ga cpx > qz, felds > ga.
cpx ga qz glass	70	Medium grained, except for large, inclusion-fille qz > cpx > ga.
cpx ga qz glass	80	Medium grained, except for large, inclusion-fille qz > ga > cpx.
plag qz glass	> 95	Minor quartz, fine grained.
plag qz glass	100	Above liquidus run.
cpx qz		Fine grained; solidus or near-solidus run; glass cpx, qz only phases identified.

36	1,390	35	cpx	qz	glass	55	Medium grained; qz > cpx.
36	1,420	20	cpx	qz	glass	75	Medium grained; qz > cpx.
36	1,450	20		qz	glass	95	Fine grained quartz only crystalline phase.
Dacite + 2.5% garnet							
27	1,200	120	cpx	felds	qz	—	Medium grained; qz > ga > felds > cpx.
27	1,350	60	cpx	ga	qz	85	Subhedral, inclusion filled garnet, rare stubby clinopyroxene, common small quartz crystals; qz > ga ≫ cpx.
27	1,370	60		ga ?	qz	95	Trace of resorbed garnet-inclusion free; minor small quartz crystals; no evidence for growth of garnet.
27	1,380	60		qz	glass	99	Rare quartz crystals; very rare resorbed, anhedral garnet fragments.

(5—30 μ) equant stubby crystals, often in aggregates. The crystal form usually distinguishes primary clinopyroxene from quench pyroxene (which is evident as "feathery" aggregates of acicular crystals). Garnet is characterized by its large crystal size (usually > 30 μ) and euhedral form. It is usually comparatively free of inclusions in compositions ranging from high-alumina olivine tholeiite to andesite but in the dacite composition garnets grown under dry conditions contain abundant inclusions (quartz mainly and some pyroxene). Quartz occurs as small crystals evenly scattered throughout the glass. It has low, negative relief and very low birefringence.

a) Crystallization at 9 kb

It has been noted elsewhere (T. H. GREEN, 1967a, b; GREEN, GREEN and RINGWOOD, 1967) that plagioclase and pyroxene are the near-liquidus phases in the high-alumina basalt and the andesite (quartz diorite) compositions at 9 kb. Similarly clinopyroxene and plagioclase are the near-liquidus phases in the basaltic andesite at 1220 and 1200° C. In the dacite composition plagioclase is the liquidus phase at 1240° C and is the only phase crystallizing until 1180° C, where it is joined by clinopyroxene and possibly quartz. Quartz is definitely present at 1100° C. Feldspar and quartz are the near-liquidus phases in the rhyodacite I composition at 1190° C and are joined by pyroxene at 1170° C.

b) Crystallization at 18 kb

In the high-alumina olivine tholeiite at 18 kb clinopyroxene is the liquidus phase at 1340° C and is the only phase to crystallize until 1280° C, where it is joined by garnet and plagioclase. These three phases continue crystallizing into the sub-solidus field. Clinopyroxene is the liquidus phase in the high-alumina quartz tholeiite at 1345° C, and is joined by plagioclase and garnet crystals at 1300° C, and these three phases are possibly joined by minor quartz at 1250° C in the sub-solidus field. Similarly in the basaltic andesite composition clinopyroxene is the near-liquidus phase at 1300° C, joined by plagioclase and garnet at 1250° C, and finally by quartz at 1200° C in the sub-solidus field. In contrast to these results described so far, the near-liquidus phases in the andesite at 18 kb 1260° C are plagioclase and garnet and these phases are joined by clinopyroxene and quartz at 1220° C. These four phases continue to crystallize into the sub-solidus field. (Note: the sub-solidus runs listed as "wet" in Table 7 have only had access to a minor amount of water — no water has been added to the sample as in the wet runs described on p. 142.) Quartz is the liquidus phase in the dacite

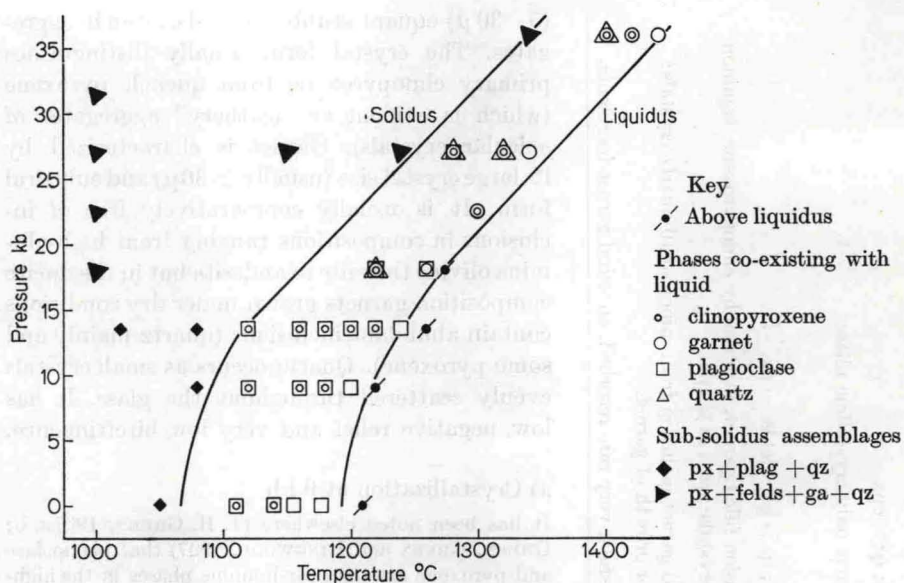


Fig. 4. Results of the dry experimental runs on the andesite composition

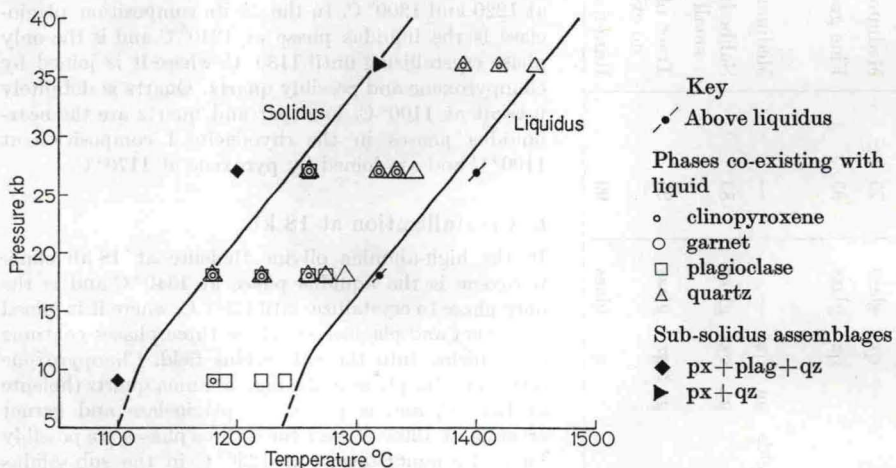


Fig. 5. Results of the dry experimental runs on the dacite composition

at 1290° C joined by plagioclase (1275° C) and then by clinopyroxene (1260° C) and finally garnet (1220° C).

c) Crystallization at 27 kb

Clinopyroxene is the liquidus phase (1435° C) in the high-alumina olivine tholeiite at 27 kb; it is joined by garnet at 1430° C and these two phases continue to crystallize together to the solidus (below 1360° C). Clinopyroxene is more common than garnet at all temperatures. A similar pattern of crystallization occurs in the high-alumina quartz tholeiite with clinopyroxene on the liquidus at 1440° C, joined by garnet at 1420° C. These phases continue

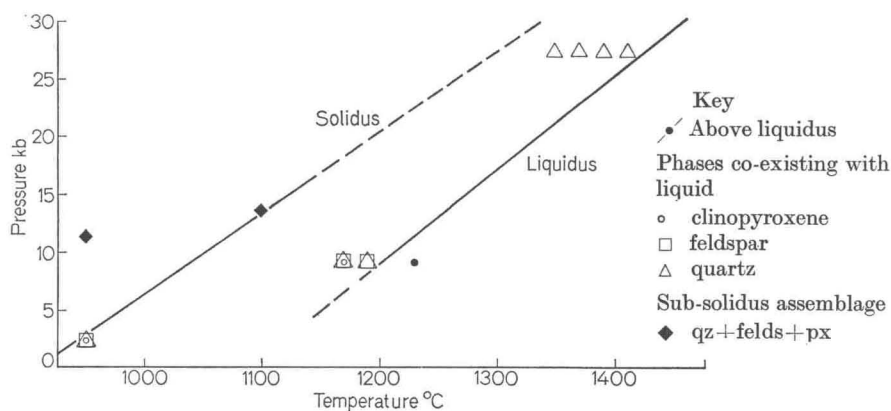


Fig. 6. Results of the experimental runs on the rhyodacite I composition

Table 9. Results of the experimental runs on the rhyodacite I (adamellite) composition

Note: Only runs carried out in this work are listed, other results given in Fig. 6 are taken from D. H. GREEN and LAMBERT (1965).

Conditions of the run			Phases present	Estimated % of glass	Comments
Pressure (kb)	Temperature (°C)	Time (mins)			
9	1,170	60	fels qz px glass	80	Moderately well crystallized feldspar, quartz; are pyroxene; qz > fels ≫ px
9	1,190	60	fels qz glass	90	Minor feldspar, quartz
9	1,230	60	glass	100	Above liquidus, all glass
27	1,350	45	qz glass	80	Moderately well crystallized; quartz only identified crystalline phase
27	1,370	40	qz glass	90	Moderately well crystallized; quartz only identified crystalline phase
27	1,390	35	qz glass	95	Moderately well crystallized; quartz only identified crystalline phase
27	1,410	25	qz glass	> 95	Rare quartz

to crystallize together at least to 1370° C. At 1300° C quartz is present in the sub-solidus field. Both garnet and clinopyroxene are the near-liquidus phases in the basaltic andesite at 1390° C. However in this case clinopyroxene is subordinate to garnet, but with increasing degree of crystallization clinopyroxene becomes the major phase (e.g. at 1380° C). These two phases are the only phases crystallizing to 1330° C, but are accompanied by quartz in the sub-solidus field (e.g. at 1300 and 1250° C). In contrast to the more basic compositions at 27 kb, in the andesite composition garnet alone is the liquidus phase at 1340° C, joined by clinopyroxene and quartz at 1320° C, and by feldspar at 1280° C. Garnet, clinopyroxene, quartz and feldspar are the sub-solidus phases in a variety of runs on the andesite from

1000–1240° C. The nature of the feldspar is uncertain, but at this pressure it is likely to be a potash feldspar, although some metastable persistence of plagioclase may occur in dry sub-solidus runs of only an hour in length. The change from plagioclase-dominated feldspar to potash feldspar probably occurs between 22.5 and 27 kb, since a marked decrease in feldspar abundance occurs in the 4 hour wet runs between these pressures (c.f. D. H. GREEN and LAMBERT, 1965).

Quartz is the liquidus phase in the dacite composition at 1350° C, joined by garnet and clinopyroxene at 1335° C, and finally by feldspar at 1260° C. The composition of the feldspar is uncertain, but it is likely to be potash-rich, as in the andesite composition. In a sub-solidus run for one hour at 1200° C only clinopyroxene, quartz and feldspar were detected; the absence of garnet suggests lack of equilibrium in this run, with some clinopyroxene and feldspar occurring metastably in place of garnet. In the rhyodacite I composition at 27 kb quartz is the liquidus phase at about 1410° C, and is the only phase crystallizing down to 1350° C.

In order to verify the presence of quartz, not garnet, as the liquidus phase in the dacite composition at 27 kb a dacite mix seeded with 2.5% of crystals of a natural pyrope-almandine garnet has been prepared. The results of the runs on this composition are given in Table 8. At 1380 and 1370° C quartz was present, together with rare resorbed fragments of garnet (< 2.5% initially added to the mix) while at 1350° C quartz and minor euhedral garnet occurred and at 1200° C these two phases are joined by feldspar and pyroxene. Thus these experiments show the stability of quartz relative to garnet as the liquidus phase in the dacite composition at 27 kb under dry conditions.

Table 10. *Electron microprobe analyses of clinopyroxenes from selected runs on the high-alumina*

Composition	High-alumina olivine tholeiite								High-alumina	
	18 kb 1,230° C 120mins (Wet ^a)	18 kb 1,260° C 120mins (Wet ^a)	18 kb 1,300° C 60mins	18 kb 1,320° C 60mins	18 kb 1,340° C 60mins	27 kb 1,430° C 25mins	27 kb 1,435° C 30mins	36 kb 1,520° C 15mins	18 kb 1,300° C 55mins	18 kb 1,330° C 45mins
Co-existing phases	ga ^b plag ^b	ga ^b	—	—	—	ga ^b	—	ga ^b	ga ^b , plag ^b	—
SiO ₂	51.3	50.9	48.3	49.0	50.0	48.5	48.0	48.6	49.0	48.0
TiO ₂	1.9	1.1	0.9	0.9	0.7	0.6	0.5	0.9	1.6	1.3
Al ₂ O ₃	13.6	10.2	12.0	10.8	9.4	12.8	12.2	14.6	13.7	12.3
FeO	8.0	4.8	5.4	5.7	5.4	4.8	4.4	6.0	8.0	6.9
MgO	10.4	14.6	14.0	14.2	15.9	13.6	14.0	10.2	11.4	13.5
CaO	15.9	17.1	15.9	16.0	16.2	15.3	15.7	14.3	14.6	15.4
Na ₂ O	1.5	1.1	1.3	1.3	1.3	2.0	1.9	2.9	1.6	1.5
$\frac{100 \text{ Mg}}{\text{Mg} + \text{Fe}}$	102.6	99.8	97.8	97.9	98.9	97.6	96.7	97.5	99.9	98.9
Formula 6[0]										
Si } Al } ^z	1.8087 0.1913	1.8324 0.1676	1.7796 0.2204	1.8059 0.1941	1.8233 0.1767	1.7836 0.2164	1.7829 0.2171	1.7921 0.2079	1.7765 0.2235	1.7609 0.2391
Al } Ti } Fe } Mg } Ca } Na }	0.3736 0.0504 0.2358 0.5469 0.6005 0.1026	0.2651 0.0299 0.1445 0.7839 0.6595 0.0766	0.3004 0.0250 0.1665 0.7692 0.6275 0.0930	0.2750 0.0251 0.1756 0.7806 0.6317 0.0930	0.2275 0.0193 0.1648 0.8647 0.6330 0.0921	0.3383 0.0166 0.1476 0.7459 0.6027 0.1428	0.3168 0.0141 0.1366 0.7755 0.6248 0.1366	0.4263 0.0250 0.1850 0.5609 0.5649 0.2074	0.3618 0.0436 0.2425 0.6164 0.5669 0.1124	0.2927 0.0359 0.2117 0.7386 0.6052 0.1067
z	2.00	2.00	2.00	2.00	2.00	2.00	2.00	2.00	2.00	2.00
x + y	1.91	1.96	1.98	1.98	2.00	1.99	2.00	1.97	1.94	1.99
AT. PROP.										
Mg	39.5	49.4	49.2	49.1	52.0	49.8	50.5	42.8	43.2	47.5
Fe	17.0	9.1	10.7	11.1	9.9	9.9	8.9	14.1	17.0	13.6
Ca	43.5	41.5	40.1	39.8	38.1	40.3	40.6	43.1	39.8	38.9

^a The procedure used for these wet runs did not involve adding water to the sample and a

^b Denotes co-existing phase analyzed.

d) Crystallization at 36 kb

Only two runs have been conducted on the high-alumina olivine tholeiite at 36 kb. Clinopyroxene and garnet are the only primary phases present in these runs. Garnet is more abundant than clinopyroxene in the near-liquidus run at 1535° C while at 1520° C clinopyroxene is the dominant phase. Similar crystallization occurs in the high-alumina quartz tholeiite composition where garnet and clinopyroxene are the near-liquidus phases at 1525° C and continue to be the only phases crystallizing at least down to 1420° C where minor quartz may be present. In the basaltic andesite composition at 36 kb garnet and clinopyroxene are the crystallizing phases in the partial melting field between 1440 and 1475° C. Garnet is the dominant primary phase at 1475° C but is subordinate to primary clinopyroxene at 1460 and 1440° C. These two phases are joined by quartz in the sub-solidus field (e.g. at 1380° C). The trend of increasing abundance of garnet as a near-liquidus phase from olivine tholeiite through quartz tholeiite to basaltic andesite continues to the andesite composition, where garnet is the liquidus phase at 1440° C. Garnet is the major crystallizing phase down to 1400° C; it is joined by clinopyroxene at 1420° C and by quartz at 1400° C; minor feldspar (probably potash-rich) is present in a near-solidus run at 1340° C. In the dacite composition quartz is the liquidus phase at 1450° C and is joined by clinopyroxene at 1420° C. These are the only phases identified down to a near-solidus run at 1320° C. The presence of garnet in 27 kb runs on this composition, and its absence at 36 kb suggests nucleation problems in crystallizing garnet at 36 kb.

olivine tholeiite, high-alumina quartz tholeiite and basaltic andesite compositions

quartz tholeiite					Basaltic andesite					
27 kb 1,385° C 35 mins	27 kb 1,400° C 30 mins	27 kb 1,420° C 20 mins	36 kb 1,490° C 15 mins	36 kb 1,510° C 10 mins	18 kb 1,250° C 60 mins	18 kb 1,280° C 60 mins	27 kb 1,360° C 40 mins	27 kb 1,390° C 35 mins	36 kb 1,460° C 20 mins	36 kb 1,475° C 15 mins
ga ^b	ga ^b plag ^b	—	ga ^b	ga ^b	ga ^b	ga ^b				
50.5	50.5	49.5	50.5	50.5	50.4	50.5	50.6	49.9	50.0	50.5
1.2	1.2	1.0	0.9	0.8	1.3	1.0	0.9	0.7	0.9	0.6
14.4	13.0	13.0	14.3	13.2	14.2	11.7	13.8	13.1	17.3	15.3
6.7	6.2	5.8	5.6	5.1	10.5	9.7	6.7	7.6	7.0	6.8
9.8	11.0	12.2	10.3	11.4	10.2	12.2	9.9	11.2	7.3	10.0
14.8	15.3	15.4	14.4	14.6	13.9	14.8	15.1	14.8	11.8	13.1
2.4	2.3	2.1	2.8	2.6	1.2	1.2	2.2	2.1	2.9	3.1
99.8	99.5	99.0	98.8	98.2	101.7	101.1	99.2	99.4	97.2	99.4
72.3	75.9	78.9	76.6	79.9	63.4	69.2	72.5	72.5	65.0	72.4
1.8181	1.8253	1.7992	1.8273	1.8369	1.8009	1.8198	1.8329	1.8150	1.8278	1.8190
0.1819	0.1747	0.2008	0.1727	0.1631	0.1991	0.1802	0.1671	0.1850	0.1722	0.1810
0.4291	0.3792	0.3563	0.4370	0.4026	0.3988	0.3166	0.4220	0.3764	0.5731	0.4684
0.0325	0.0326	0.0273	0.0246	0.0219	0.0352	0.0541	0.0246	0.0192	0.0248	0.0162
0.2016	0.2172	0.1763	0.1694	0.1552	0.3137	0.2924	0.2029	0.2313	0.2140	0.2048
0.5262	0.5930	0.6613	0.5558	0.6184	0.5435	0.6555	0.5349	0.6075	0.3979	0.5371
0.5708	0.5924	0.5997	0.5582	0.5688	0.5322	0.5713	0.5861	0.5767	0.4621	0.5055
0.1675	0.1612	0.1481	0.1966	0.1832	0.0833	0.0840	0.1546	0.1482	0.2057	0.2165
2.00	2.00	2.00	2.00	2.00	2.00	2.00	2.00	2.00	2.00	2.00
1.93	1.98	1.97	1.94	1.95	1.91	1.97	1.93	1.96	1.88	1.95
40.5	43.2	46.0	43.3	46.0	39.1	43.2	40.4	42.9	37.0	43.1
15.5	13.7	12.3	13.2	11.6	22.6	19.2	15.3	16.3	19.9	16.4
44.0	43.1	41.7	43.5	42.4	38.3	37.6	44.3	40.8	43.1	40.5

dried pyrophyllite spacer was used.

Table 11. *Electron microprobe analyses of garnets from selected runs on the high-alumina*

Composition	High-alumina olivine tholeiite					High-alumina quartz tholeiite					
	18 kb 1,230°C 120 mins (Wet)	18 kb 1,260°C 120 mins (Wet)	27 kb 1,400°C 40 mins	27 kb 1,430°C 25 mins	36 kb 1,520°C 15 mins	18 kb 1,300°C 55 mins	27 kb 1,385°C 35 mins	27 kb 1,400°C 30 mins	27 kb 1,420°C 20 mins	36 kb 1,490°C 15 mins	36 kb 1,510°C 10 mins
Conditions of run											
Co-existing phase	cpx ^b plag ^b	cpx ^b	cpx	cpx ^b	cpx ^b	cpx ^b , plag ^b	cpx ^b	cpx ^b	cpx ^b	cpx ^b	cpx ^b
SiO ₂	41.0	41.3	39.0	38.5	40.0	39.0	39.0	39.0	39.5	39.0	39.5
TiO ₂	1.8	0.8	1.1	0.7	1.2	1.5	1.5	1.8	1.4	1.3	1.3
Al ₂ O ₃	22.0	22.8	20.4	21.6	22.8	22.9	22.6	23.0	23.0	22.7	23.1
FeO	17.7	9.1	14.3	10.2	13.8	15.2	14.8	14.4	12.9	13.8	12.1
MnO	0.4	0.4	0.4	0.3	0.4	0.5	0.4	0.5	0.4	0.4	0.4
MgO	12.6	17.9	13.4	16.9	13.3	11.6	10.9	11.7	12.8	11.4	12.4
CaO	7.8	6.7	7.9	7.6	8.9	7.2	7.9	7.9	7.7	8.3	8.1
$\frac{100 \text{ Mg}}{\text{Mg} + \text{Fe}}$	103.3	99.0	96.5	95.8	100.4	97.9	97.1	98.3	97.7	96.9	96.9
$\frac{100 \text{ Mg}}{\text{Mg} + \text{Fe}}$	55.9	77.8	62.6	74.7	63.2	57.6	56.8	59.2	63.9	59.6	64.6
Mol. Prop.											
Ti-andradite	4.7	2.1	3.1	1.8	3.3	4.7	4.8	5.2	4.2	4.0	4.0
Grossularite	15.1	15.0	17.1	17.5	19.8	15.5	17.8	16.9	17.3	19.5	19.1
Pyrope	44.4	63.9	49.0	59.8	48.1	45.3	43.4	45.4	49.6	45.0	49.1
Almandine	35.0	18.2	29.4	20.3	28.0	33.4	33.1	31.4	28.0	30.6	26.9
Spessartine	0.8	0.8	0.8	0.6	0.8	1.1	0.9	1.1	0.9	0.9	0.9

^a Denotes calculated composition. ^b Denotes co-existing phase analyzed.

Analytical Data

Analyses of clinopyroxene, garnet and plagioclase crystallized in the high pressure runs are given in the accompanying tables (Tables 10—12).

a) Clinopyroxenes

Analyses of clinopyroxenes crystallizing from compositions ranging from high-alumina olivine tholeiite to dacite are given in Table 10, together with the chemical formula calculated on the basis of 6 oxygen atoms per formula unit. These analyses show an increase in soda content of the pyroxene with increasing pressure, and an increase in the alumina content and a decrease in the $\frac{\text{Mg}}{\text{Mg} + \text{Fe}}$ ratio with increasing degree of crystallization at a specific pressure.

For comparable degrees of crystallization there is an increase in alumina in tetrahedral co-ordination in the pyroxene with increasing pressure (e.g. compare analyses of clinopyroxene at 9 kb with 8.8% Al₂O₃, GREEN, 1967a, with clinopyroxene at 18 kb with 9.4—12.0% Al₂O₃, Table 10; both pyroxenes are from high-alumina olivine tholeiite), until the pyroxene is joined by garnet (e.g. compare analyses of clinopyroxene from high-alumina quartz tholeiite co-existing with garnet near the liquidus at 27 and 36 kb with the analysis of a near-liquidus clinopyroxene at 18 kb). The overall alumina content of the clinopyroxene may continue to rise with increasing pressure, without obtaining more alumina in tetrahedral co-ordination, because the soda content is also increasing with increasing pressure.

b) Garnets (Table 11)

The garnets are all dominantly pyrope-almandine with a subordinate grossular-Ti-andradite component and a minor spessartine component. In general, for approximately equivalent pressures and degrees of crystallization the garnets become more almandine-rich as the parent composition becomes more acid (e.g. as it changes from high-alumina olivine tholeiite to rhyodacite near-liquidus garnet at 27 kb increases in almandine content from 33.5 mol. per cent to 67.1 mol per cent; analysis of rhyodacite garnet given in T. H. GREEN and RING-

olivine tholeiite, high-alumina quartz tholeiite, basaltic andesite, andesite, dacite compositions

Basaltic andesite					Andesite				Dacite			
18 kb 1,250°C 60mins	27 kb 1,360°C 40mins	27 kb 1,390°C 35mins	36 kb 1,460°C 20mins	36 kb 1,475°C 15mins	22.5 kb 1,300°C 60mins	27 kb 1,340°C 60mins	36 kb 1,420°C 20mins	36 kb 1,440°C 15mins	27 kb 960°C 60mins Wet	27 kb 1,040°C 60mins Wet	27 kb 1,100°C 60mins Wet	27 kb 1,140°C 60mins Wet
cpx ^b , plag ^b	cpx ^b	cpx ^b	cpx ^b	cpx ^b	—	—	cpx ^b	—	cpx, ky, qz	cpx, qz	cpx ^b	—
38.0	38.2	38.3	38.0	38.1	39.2	39.1	39.0	39.9	38.8	39.8	39.9	38.9
1.5	1.6	1.1	1.2	1.0	1.1	1.1	1.0	0.9	2.1	2.3	1.9	1.6
22.1	22.3	22.5	22.2	22.6	22.2	22.4	22.7	22.9	20.9	21.4	22.3	22.3
19.1	17.8	15.9	18.8	15.7	17.6	17.7	18.4	16.8	25.5	22.8	22.1	20.9
0.4	0.3	0.3	0.3	0.3	0.4	0.4	0.4	0.4	0.3	0.3	0.3	0.3
10.0	10.3	11.9	9.6	11.4	10.8	10.7	10.5	11.0	4.3	7.3	8.2	9.4
7.1	8.2	7.9	8.4	8.4	7.0	7.4	7.4	7.0	11.9	10.7	9.7	9.3
98.2	98.7	97.9	98.5	97.5	98.3	98.8	99.4	98.9	103.8	104.6	104.4	102.7
48.3	50.8	57.1	47.6	56.4	52.2	51.9	50.4	53.9	23.1	36.3	39.8	44.5
4.6	4.6	3.1	3.5	2.9	3.2	3.2	2.9	2.6	5.9	6.3	5.1	4.3
15.0	17.7	18.2	19.4	19.9	16.2	17.1	17.2	17.0	25.4	21.2	20.0	19.6
38.4	39.1	44.6	36.4	43.2	41.6	40.9	39.8	42.8	15.7	26.1	29.6	33.6
41.1	38.0	33.5	40.1	33.4	38.1	37.9	39.2	36.7	52.4	45.8	44.7	41.9
0.9	0.6	0.6	0.6	0.6	0.9	0.9	0.9	0.9	0.6	0.6	0.6	0.6

WOOD, in press). The $\frac{\text{Mg}}{\text{Mg} + \text{Fe}}$ ratio for the garnets is invariably lower than this ratio in co-existing clinopyroxenes. In any particular composition the lime content of the garnet increases with increasing pressure, for similar degrees of crystallization at the various pressures under comparison.

c) Plagioclase (Table 12)

Only a few plagioclase analyses are listed in Table 12 since more detailed work involving plagioclase is dealt with elsewhere (T. H. GREEN, 1967a, b and in preparation). The most noteworthy feature of the analyses given in Table 12 is the increase in albite content of the plagioclase crystallizing from the basaltic andesite under dry conditions, as the pressure is increased from 9—18 kb.

Summary of the Most Significant Results

1. The near-liquidus phases in the basalt to dacite compositions change from plagioclase-pyroxene dominated at 0—18 kb to pyroxene-garnet dominated at 27—36 kb.
2. The pyroxene crystallizing at high pressure contains more alumina and less silica than the low pressure pyroxene. This contributes to the subsilicic character of the near-liquidus phases crystallizing at high pressures.
3. The proportion of garnet relative to pyroxene increases as the pressure is increased from 27—36 kb.
4. The proportion of garnet relative to pyroxene as a near-liquidus phase increases as the bulk composition becomes more acidic.
5. The almandine content of the garnet increases as the bulk composition changes from basalt to rhyodacite.

Table 12. *Electron microprobe analyses of plagioclases from selected runs on the high-alumina olivine tholeiite, high-alumina quartz tholeiite and basaltic andesite compositions*

Composition	High-alumina	High-alumina	Basaltic andesite	
	olivine tholeiite	quartz tholeiite		
Conditions of Run	18 kb 1,230°C 2 hrs Wet ^c	18 kb 1,300°C 55 mins	9 kb 1,200°C 60 mins	18 kb 1,250°C 60 mins
Co-existing phases	cpx ^b , ga ^b	cpx ^b , ga ^b	cpx	cpx ^b , ga ^b
SiO ₂	57.5 ^a (56.0)	56.6	55.9	58.0
Al ₂ O ₃	26.3	26.8	27.5	26.6
CaO	9.0	9.5	10.7	8.5
Na ₂ O	6.5 ^a (6.1)	6.0 ^a (5.8)	5.3 ^a (5.2)	6.5 ^a (5.9)
K ₂ O	0.08	0.3	0.3	0.5
	99.4	99.2	99.7	100.1
Mol. Prop.				
Or	0.5	1.7	1.8	2.9
Ab	56.3	52.4	46.6	56.3
An	43.2	46.9	51.6	40.8

^a Denotes calculated content; bracketed values following calculated contents are the measured contents.

^b Denotes co-existing phase analyzed.

^c Water not added to sample.

6. Andesite rather than more acidic dacite or rhyodacite has the lowest liquidus temperature at 27–36 kb. This is best illustrated in Figs. 7 and 8.

7. The liquidus phase changes from garnet to quartz as the bulk composition changes from andesite to dacite (Fig. 8).

Interpretation of Results

In Fig. 7 the liquids have been extrapolated at their 18–36 kb gradients to a pressure of 50 kb corresponding to a depth of about 160 kms. The andesite liquidus falls below the dacite and rhyodacite liquids and above the tholeiite solidus at high pressures. The higher liquids of the dacite and rhyodacite and the presence of quartz on the liquidus of these two compositions at high pressure under dry conditions indicate that at depth andesite is a lower melting fraction than the more acid compositions. Thus at depths of 100–150 kms fractional crystallization of basalt and basaltic andesite by separation of garnet and pyroxene will cause the composition of the liquid fractionate to move towards that of an andesite. This conclusion is emphasized in Fig. 8 where the extrapolated liquids and sequence of crystallization of phases under dry conditions at 30 kb are plotted. This shows clearly that the andesite composition lies in a marked thermal valley, and that there is a change in liquidus phase from garnet to quartz between the andesite and dacite compositions.

The importance of garnet and clinopyroxene as the co-crystallizing phases in the basaltic compositions is that because of their sub-silicic character, they provide a highly efficient means of enriching the fractionating liquid in silica and alkalis. A sharp rise in Fe/Mg ratio due to crystallization of low Fe/Mg clinopyroxene is precluded by the simultaneous crystallization of almandine-rich garnet. Thus

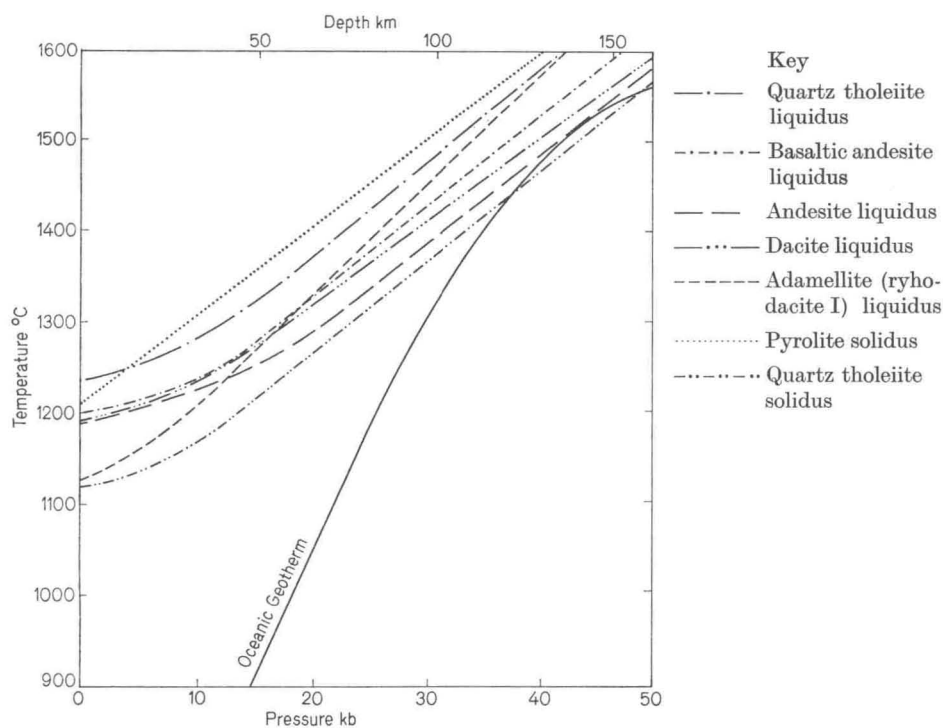


Fig. 7. Combined liquidus plot for the compositions studied under dry conditions

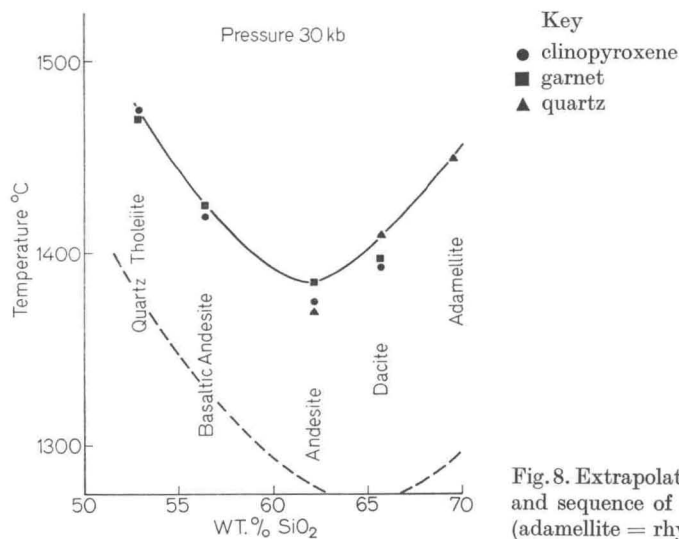


Fig. 8. Extrapolated liquidus temperatures and sequence of crystallization at 30 kb (adamellite = rhyodacite I)

the liquids formed from basaltic compositions by the fractional crystallization of garnet and pyroxene follow the calc-alkali trend (see Tables 16—20 and Figs. 10 and 11).

The results have been discussed above in terms of fractional crystallization at high pressure. However the same observations apply to the reverse case of fractional melting of a basaltic composition at high pressures where the sub-solidus mineral assemblage consists of garnet, pyroxene and quartz. It is envisaged that varying degrees of fractional melting can give rise to liquids of typical calc-alkaline descent, e.g. basaltic andesite and andesite. The residuum is composed of varying proportions of garnet and clinopyroxene, depending on the degree of melting. Thus at depths of 100–150 kms if the temperature is sufficiently

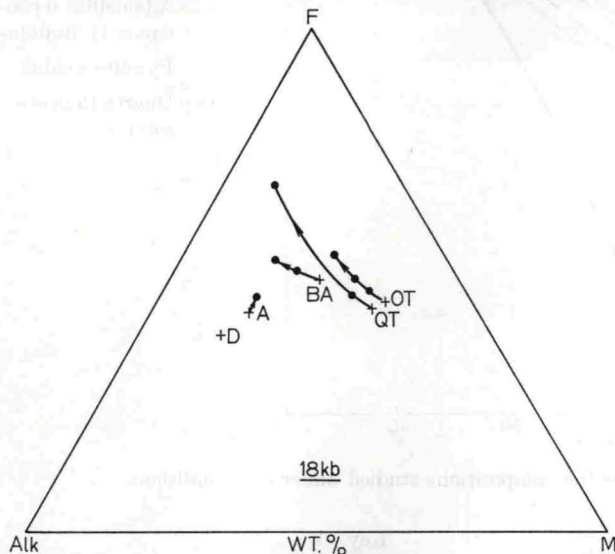


Fig. 9. Experimentally determined fractionation trends at 18 kb shown on an FMA plot
 Note: In this and subsequent FMA diagrams: $F = \text{FeO} + 0.9 \text{Fe}_2\text{O}_3$; $M = \text{MgO}$; $\text{Alk} = \text{Na}_2\text{O} + \text{K}_2\text{O}$; $\text{OT} = \text{high-alumina olivine tholeiite}$; $\text{QT} = \text{high-alumina quartz tholeiite}$; $\text{BA} = \text{basaltic andesite}$; $A = \text{andesite}$; $D = \text{dacite}$

high for partial melting of the tholeiite to take place under dry conditions, the early forming liquid will trend towards an andesitic composition rather than more acid compositions. The degree of melting will to some extent govern the Fe/Mg ratio of the liquids obtained, since the Fe/Mg ratio of the garnet and clinopyroxene (as well as the relative proportions of garnet and clinopyroxene) varies with temperature. Thus a family of compositions with some variation in Fe/Mg ratio, but nevertheless still with an overall calc-alkali trend showing only slight iron enrichment relative to magnesium, may be obtained by the fractional melting of basalt under dry conditions at high pressure. For degrees of melting less than those required to produce andesite (40–50% melting), but nevertheless still large enough to allow magma segregation (probably at least 20% melting required), the liquids produced will be enriched in alkalis, but not silica, for dry melting conditions. These alkali-enriched liquids may have affinities with some oversaturated syenites found associated with calc-alkaline rocks (JOPLIN, 1965). The residuum remaining after derivation of such compositions will consist mainly of garnet and pyroxene, together with some quartz.

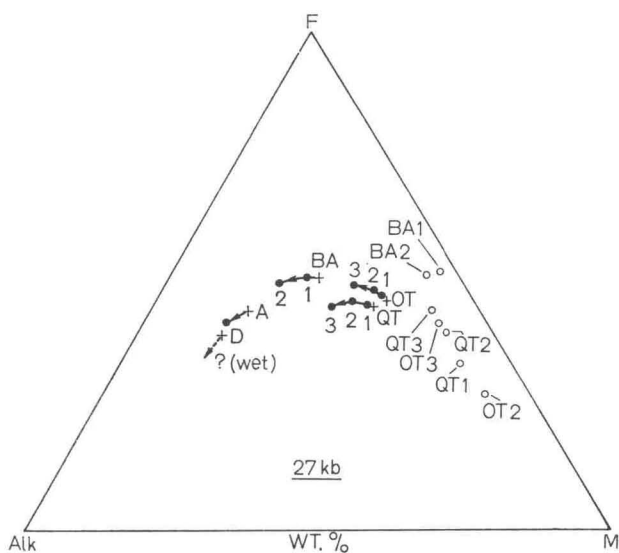


Fig. 10. FMA plot showing experimentally determined fractionation trends at 27 kb. The encircled points represent the plots of the residua — the numbers correspond to the numbered points on the fractionation trends

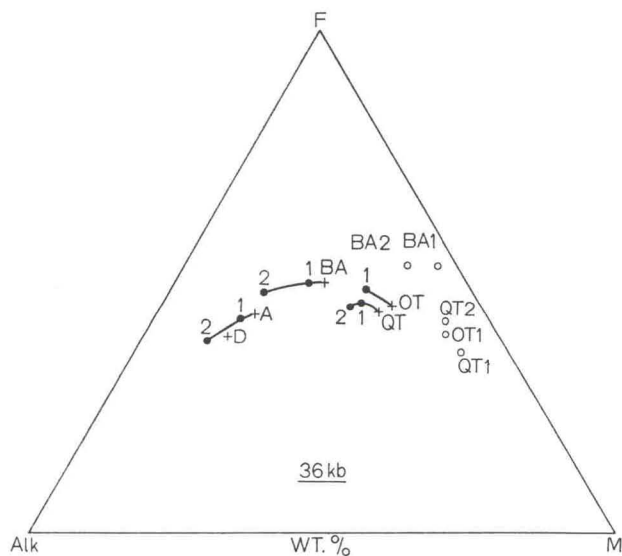


Fig. 11. FMA plot showing experimentally determined fractionation trends at 36 kb. The encircled points represent the plots of the residua — the numbers correspond to the numbered points on the fractionation trends

Calculation of Fractionation Trends

The calculated liquid fractionate compositions derived from the various initial compositions are listed in Tables 13—20, together with the compositions of the crystalline residua. At 18 kb, the liquids show minor enrichment in silica, alkalis

Table 13. *Calculated compositions of liquid fractionates and crystalline residua derived from the high-alumina olivine tholeiite composition at 18 kb*

Temperature	1,340° C	1,320° C	1,300° C	1,260° C (Wet)	1,230° C (Wet)	
Nature and estimated % of crystals	Initial liquid	10% cpx	20% cpx	30% cpx	20% cpx 2% ga	30% cpx 15% ga 5% plag
<i>Liquid fractionate</i>						
SiO ₂	50.3	50.3	50.4 ^a	50.8 ^a	50.4	52.9 ^a
TiO ₂	1.7	1.8	1.9	2.0	1.9	1.8
Al ₂ O ₃	17.0	17.8	18.5	19.0	18.6	16.7
Fe ₂ O ₃	1.5	1.7	1.9	2.1	1.9	3.0
FeO	7.6	7.8	8.0	8.5	8.3	6.3
MnO	0.16	0.18	0.2	0.23	0.2	0.2
MgO	7.8	6.9	6.1	5.0	5.8	5.6
CaO	11.4	10.9	10.2	9.3	10.1	9.9
Na ₂ O	2.8	3.0	3.2	3.4	3.3	4.0
K ₂ O	0.18	0.2	0.2	0.26	0.23	0.3
	100.4	100.6	100.6	100.6	100.7	100.7
Mol Prop						
100 MgO	60.7	57.0	52.9	46.2	50.8	52.6
MgO + FeO _{Total}						
<i>CIPW norm</i>						
Qz	—	—	—	—	—	0.8
Or	1.1	1.2	1.3	1.6	1.3	1.8
Ab	23.7	25.3	27.1	28.8	27.9	33.9
An	33.3	34.5	35.4	35.7	35.2	26.7
Diop	18.9	15.9	12.3	8.6	12.2	18.1
Hyp	11.9	12.3	14.1	18.8	13.1	11.7
Ol	6.2	5.4	4.0	0.3	4.6	—
Mt	2.2	2.5	2.8	3.0	2.8	4.4
Ilm	3.2	3.4	3.6	3.8	3.6	3.4
<i>Crystal residuum</i>						
SiO ₂		50.0	49.9 ^a	49.2 ^a	50.0	47.7 ^a
TiO ₂		0.7	0.9	0.9	1.1	1.6
Al ₂ O ₃		9.4	11.1	12.3	11.3	17.3
FeO		5.4	5.8	5.6	5.2	8.5
MnO		—	—	—	0.04	0.1
MgO		15.9	14.6	14.4	14.9	10.0
CaO		16.2	16.4	16.3	16.2	12.8
Na ₂ O		1.3	1.3	1.3	1.0	1.6
K ₂ O		—	—	—	—	tr
		98.9	100.0	100.0	99.7	99.6
Mol prop.						
100 MgO		84.0	81.8	82.1	83.6	67.7
MgO + FeO						

^a Denotes compositions determined from analyses calculated in the manner described on p. 116.

Table 14. Calculated compositions of liquid fractionates and crystalline residua derived from the high-alumina quartz tholeiite and basaltic andesite compositions at 18 kb

Composition	High-alumina quartz tholeiite			Basaltic andesite		
		1,330° C	1,300° C		1,280° C	1,250° C
Temperature						
Nature and estimated % of crystals	Initial liquid	15% cpx	50% cpx 10% plag 5% ga	Initial liquid	10% cpx	25% cpx 10% plag 1% ga
<i>Liquid fractionate</i>						
SiO ₂	52.9	53.8	58.1	56.4	57.1	58.8
TiO ₂	1.5	1.5	1.8	1.4	1.4	1.7
Al ₂ O ₃	16.9	17.7	17.8	16.6	17.1	15.9
Fe ₂ O ₃	0.3	0.4	0.9	3.0	3.3	4.7
FeO	7.9	8.1	9.0	5.7	5.3	4.5
MnO	0.2	0.2	0.5	0.1	0.1	0.2
MgO	7.0	5.9	2.1	4.3	3.4	2.6
CaO	10.0	9.0	4.0	8.5	7.8	6.4
Na ₂ O	2.7	2.9	3.7	3.0	3.2	3.2
K ₂ O	0.6	0.7	1.6	1.0	1.1	1.5
	100.0	100.2	99.5	100.0	99.8	99.5
<i>Mol. Prop.</i>						
	$\frac{100 \text{ MgO}}{\text{MgO} + \text{FeO}_{\text{Total}}}$					
	60.4	55.4	27.6	47.7	42.2	34.8
<i>CIPW norm</i>						
Qz	1.3	3.0	13.1	10.7	12.4	17.6
Or	3.5	4.2	9.4	5.9	6.5	8.8
Ab	22.8	24.6	30.7	25.4	27.1	27.1
An	32.2	33.2	19.9	28.9	29.0	24.6
Diop	14.2	9.4	2.7	10.8	14.7	5.6
Hyp	22.6	22.5	19.0	11.3	9.5	5.7
Ol	—	—	—	—	—	—
Mt	0.4	0.6	1.3	4.3	4.8	6.8
Ilm	2.8	2.8	3.4	2.7	2.7	3.2
<i>Crystal residuum</i>						
SiO ₂		50.1	48.0		50.5	52.1
TiO ₂		1.4	1.3		1.0	1.0
Al ₂ O ₃		16.4	12.3		11.7	17.8
FeO		7.3	6.9		9.7	7.8
MnO		tr	—		—	0.1
MgO		9.7	13.5		12.2	7.3
CaO		13.2	15.4		14.8	12.2
Na ₂ O		2.2	1.4		1.2	2.6
K ₂ O		0.1	—		—	0.1
		100.4	98.8		101.1	101.0
<i>Mol Prop.</i>						
	$\frac{100 \text{ MgO}}{\text{MgO} + \text{FeO}}$					
		70.3	77.7		69.2	62.5

Table 15. *Calculated approximate composition of liquid fractionate and crystalline residuum from the andesite composition at 18 kb*

Note: Suitable electron microprobe analyses of garnet and plagioclase could not be obtained at 18 kb. However as an approximation the composition of the garnet from a 22.5 kb run is taken. The composition of the plagioclase is estimated as $Or_5Ab_{65}An_{30}$ by comparison with plagioclase in the basaltic andesite at 18 kb and assuming that the albite enrichment trend with increasing pressure continues to 18 kb in the plagioclases crystallizing from the andesite (see p. 129).

Temperature		1,260° C		Temperature		1,260° C	
Nature and estimated % of crystals	Initial liquid	12% plag	3% ga	Nature and estimated % of crystals	Initial liquid	12% plag	3% ga
<i>Liquid fractionate</i>				<i>CIPW norm</i>			
SiO ₂	62.2	62.8		Qz	15.5	18.7	
TiO ₂	1.1	1.3		Or	13.6	15.4	
Al ₂ O ₃	17.3	16.4		Ab	27.9	22.0	
Fe ₂ O ₃	0.3	0.4		An	25.7	25.4	
FeO	5.9	6.3		Diop	0.2	0.7	
MnO	0.1	0.1		Hyp	14.8	14.8	
MgO	2.4	2.4		Ol	—	—	
CaO	5.2	5.3		Mt	0.4	0.6	
Na ₂ O	3.3	2.6		Ilm	2.1	2.5	
K ₂ O	2.3	2.6		<i>Crystal residuum</i>			
Mol. Prop.	100.1	100.2		SiO ₂		58.9	
100 MgO				TiO ₂		0.2	
$\frac{MgO + FeO_{Total}}$	41.0	39.1		Al ₂ O ₃		22.5	
				FeO		3.5	
				MnO		0.1	
				MgO		2.2	
				CaO		4.4	
				Na ₂ O		7.1	
				K ₂ O		0.8	
				Mol Prop.		99.7	
				100 MgO			
				$\frac{MgO + FeO}$		52.9	

and alumina and also in iron (except where crystallization is greater than 30%) but there is marked depletion in magnesia. Thus the fractionating liquids show a large drop in the $\frac{Mg}{Mg + Fe}$ ratio. In contrast to the trends at 18 kb, the liquid fractionation trends at 27–36 kb (Tables 16–20) show significant enrichment in silica and alkalis, alumina remains approximately constant, and iron and magnesium are both depleted. The $\frac{Mg}{Mg + Fe}$ ratio shows a slight decrease, so that there is some iron enrichment relative to magnesia. This effect is probably accentuated by the experimental conditions where there is some iron loss to the platinum capsule during a run. This factor will mean that the iron content of the mafic phases as analyzed will be slightly less than expected for similar crystals in equilibrium with a melt without iron loss.

Table 16. Calculated compositions of liquid fractionates and crystalline residua derived from the high-alumina olivine tholeiite composition at 27 kb

Temperature		1,435° C	1,430° C	1,400° C
Nature and estimated % of crystals	Initial litquid	5% cpx	8% cpx 2% ga	25% cpx ^b 10% ga
<i>Liquid fractionate</i>				
SiO ₂	50.3	50.4	50.6 ^a	52.0 ^a
TiO ₂	1.7	1.8	1.8	2.0
Al ₂ O ₃	17.0	17.3	17.2	17.1
Fe ₂ O ₃	1.5	1.6	1.7	2.3
FeO	7.6	7.8	7.8	6.9
MnO	0.16	0.17	0.17	0.18
MgO	7.8	7.5	7.1	6.1
CaO	11.4	11.2	11.1	10.5
Na ₂ O	2.8	2.8	2.9	3.3
K ₂ O	0.18	0.2	0.2	0.28
	100.4	100.8	100.6	100.7
Mol. Prop.				
$\frac{100 \text{ MgO}}{\text{MgO} + \text{FeO}_{\text{Total}}}$	60.7	59.2	57.7	54.7
<i>CIPW norm</i>				
Qz	—	—	—	1.1
Or	1.1	1.2	1.2	1.7
Ab	23.7	23.7	24.6	27.9
An	33.3	34.1	33.3	31.0
Diop	18.9	17.5	17.7	17.1
Hyp	11.9	13.6	14.2	14.7
Ol	6.2	5.0	3.7	—
Mt	2.2	2.4	2.5	3.3
Ilm	3.2	3.4	3.4	3.8
<i>Crystal residuum</i>				
SiO ₂		48.0	48.0	47.2
TiO ₂		0.5	0.6	1.1
Al ₂ O ₃		12.2	15.1	16.8
FeO		4.4	5.9	8.9
MnO		—	0.04	0.1
MgO		14.0	14.6	11.0
CaO		15.7	14.1	13.0
Na ₂ O		1.9	1.7	1.8
K ₂ O		—	—	—
		96.7	100.0	99.9
Mol. prop.				
$\frac{100 \text{ MgO}}{\text{MgO} + \text{FeO}}$		85.0	81.5	68.8

^a Denotes compositions determined from analyses calculated in the manner described on p. 116.

^b This pyroxene could not be analyzed and is assumed to be similar in composition to the pyroxene crystallizing from the high-alumina quartz tholeiite at 27 kb, 1,385° C; the degree of crystallization is similar for this temperature.

Table 17. *Calculated compositions of liquid fractionates and crystalline residua derived from the high-alumina quartz tholeiite composition at 27 kb*

Temperature	1,420° C	1,400° C	1,385° C	
Nature and estimated % of crystals	Initial liquid	5% cpx 1% ga	15% cpx 5% ga	25% cpx 10% ga
<i>Liquid fractionate</i>				
SiO ₂	52.9	53.2	54.2	56.0
TiO ₂	1.5	1.5	1.5	1.6
Al ₂ O ₃	16.9	17.0	17.3	17.0
Fe ₂ O ₃	0.3	0.3	0.4	0.5
FeO	7.9	8.0	7.8	7.3
MnO	0.2	0.2	0.2	0.2
MgO	7.0	6.7	6.0	5.3
CaO	10.0	9.7	9.1	8.5
Na ₂ O	2.7	2.8	2.9	3.4
K ₂ O	0.6	0.6	0.7 ₅	0.9
	100.0	100.0	100.1 ₅	100.7
Mol. prop.				
100 MgO				
MgO + FeO _{Total}	60.4	59.1	56.7	54.9
<i>CIPW norm</i>				
Qz	1.3	1.7	3.4	4.7
Or	3.5	3.6	4.5	5.4
Ab	22.8	23.7	24.6	28.8
An	32.2	32.0	31.9	28.4
Diop	14.2	13.1	10.9	11.3
Hyp	22.6	22.5	21.5	18.4
Ol	—	—	—	—
Mt	0.4	0.4	0.6	0.7
Ilm	2.8	2.9	2.9	3.0
<i>Crystal residuum</i>				
SiO ₂		47.9	47.6	47.3
TiO ₂		1.1	1.4	1.3
Al ₂ O ₃		14.7	15.5	16.7
FeO		7.0	8.3	9.0
MnO		0.1	0.1	0.1
MgO		12.3	11.2	10.1
CaO		14.1	13.5	12.8
Na ₂ O		1.8	1.7	1.7
K ₂ O		—	—	—
		99.0	99.1	99.0
Mol. prop.				
100 MgO				
MgO + FeO		75.8	70.6	66.7

The fractionation trends are illustrated diagrammatically by plotting on the familiar FMA diagram, frequently used to demonstrate fractionation trends of the calc-alkaline series (Figs. 9—11). The trend in fractionation observed at

Table 18. Calculated compositions of liquid fractionates and crystalline residua derived from the basaltic andesite and andesite compositions at 27 kb

Composition	Basaltic andesite			Andesite	
		1,390° C	1,360° C	1,340° C	
Temperature					
Nature and estimated % of crystals	Initial liquid	4% ga 2% cpx	9% ga 11% cpx	Initial liquid	5% ga
<i>Liquid fractionate</i>					
SiO ₂	56.4	57.2 ^a	59.2	62.2	63.4
TiO ₂	1.4	1.4	1.4	1.1	1.1
Al ₂ O ₃	16.6	16.4	16.3	17.3	17.0
Fe ₂ O ₃	3.0	3.2	3.7	0.3	0.3
FeO	5.7	5.2	4.2	5.9	5.3
MnO	0.1	0.1	0.1	0.1	0.1
MgO	4.3	3.8	2.9	2.4	2.0
CaO	8.5	8.4	7.6	5.2	5.1
Na ₂ O	3.0	3.1	3.4	3.3	3.5
K ₂ O	1.0	1.1	1.3	2.3	2.4
	100.0	99.9	100.1	100.1	100.2
Mol. prop.					
$\frac{100 \text{ MgO}}{\text{MgO} + \text{FeO}_{\text{Total}}}$	47.7	45.6	40.8	41.0	39.0
<i>CIPW norm</i>					
Qz	10.7	12.5	15.3	15.5	16.7
Or	5.9	6.0	7.7	13.6	14.2
Ab	25.4	26.2	28.8	27.9	29.7
An	28.9	27.8	25.4	25.7	23.6
Diop	10.8	11.1	9.8	0.2	1.5
Hyp	11.3	8.9	5.0	14.8	12.1
Ol	—	—	—	—	—
Mt	4.3	4.6	5.4	0.4	0.4
Ilm	2.7	2.7	2.7	2.1	2.1
<i>Crystal residuum</i>					
SiO ₂		43.4	45.0		39.1
TiO ₂		0.9	1.2		1.1
Al ₂ O ₃		19.1	17.6		22.4
FeO		13.4	11.7		17.7
MnO		0.2	0.2		0.4
MgO		11.9	10.1		10.7
CaO		10.4	12.0		7.4
Na ₂ O		0.7	1.2		—
K ₂ O		—	—		—
		100.0	99.0		98.8
Mol. prop.					
$\frac{100 \text{ MgO}}{\text{MgO} + \text{FeO}}$		61.3	60.6		51.9

^a Denotes compositions determined from analyses calculated in the manner described on p. 116.

Table 19. *Calculated compositions of liquid fractionates and crystalline residua derived from the high-alumina olivine tholeiite and high-alumina quartz tholeiite compositions at 36 kb*

Compositions	High-alumina olivine tholeiite		High-alumina quartz tholeiite		
	1,520° C		1,510° C	1,490° C	
Nature and estimated % of crystals	Initial liquid	20% cpx 10% ga	Initial liquid	10% cpx 5% ga	15% cpx 10% ga
<i>Liquid fractionate</i>					
SiO ₂	50.3	51.9 ^a	52.9	53.9 ^a	55.1 ^a
TiO ₂	1.7	2.0	1.5	1.6	1.6
Al ₂ O ₃	17.0	16.8	16.9	17.0	16.7
Fe ₂ O ₃	1.5	2.1	0.3	0.4	0.4
FeO	7.6	7.1	7.9	7.9	7.4
MnO	0.16	0.17	0.2	0.2	0.2
MgO	7.8	6.3	7.0	6.1	5.6
CaO	11.4	10.8	10.0	9.5	9.2
Na ₂ O	2.8	3.1	2.7	2.9	3.0
K ₂ O	0.18	0.26	0.6	0.7	0.8
	100.4	100.5	100.0	100.2	100.0
<i>Mol. Prop.</i>					
100 MgO					
MgO + FeO _{Total}	60.7	55.5	60.4	56.8	56.3
<i>CIPW norm</i>					
Qz		1.4	1.3	2.9	4.9
Or	1.1	1.6	3.5	4.2	4.8
Ab	23.7	26.2	22.8	24.6	25.4
An	33.3	31.2	32.2	31.3	29.7
Diop	18.9	18.2	14.2	12.9	13.0
Hyp	11.9	15.2	22.6	20.8	18.6
Ol	6.2	—	—	—	—
Mt	2.2	3.0	0.4	0.6	0.6
Ilm	3.2	3.8	2.8	3.0	3.0
<i>Crystal residuum</i>					
SiO ₂		46.6		47.5	46.4
TiO ₂		1.0		1.0	1.1
Al ₂ O ₃		17.4		16.4	17.6
FeO		8.7		7.9	9.4
MnO		0.1		0.1	0.2
MgO		11.4		12.3	11.2
CaO		12.9		13.0	12.4
Na ₂ O		2.0		1.8	1.7
K ₂ O		—		—	—
		100.1		100.0	100.0
<i>Mol. prop.</i>					
100 MgO					
MgO + FeO		70.0		73.5	68.0

^a Denotes compositions determined from analyses calculated in the manner described on p. 116.

Table 20. Calculated compositions of liquid fractionates and crystalline residua derived from the basaltic andesite and andesite compositions at 36 kb

Composition	Basaltic andesite			Andesite		
		1,475° C	1,460° C		1,440° C	1,420° C
Nature and estimated % of crystals	Initial liquid	6% ga 2% cpx	12% ga 20% cpx	Initial liquid	3% ga	10% ga tr. cpx (neglected)
<i>Liquid fractionate</i>						
SiO ₂	56.4	57.6 ^a	61.2 ^a	62.2	63.0	64.8
TiO ₂	1.4	1.4	1.6	1.1	1.1	1.1
Al ₂ O ₃	16.6	16.3	15.3	17.3	17.1	16.7
Fe ₂ O ₃	3.0	3.3	4.4	0.3	0.3	0.3
FeO	5.7	5.0	2.8	5.9	5.6	4.5
MnO	0.1	0.1	0.1	0.1	0.1	0.1
MgO	4.3	3.7	2.3	2.4	2.1	1.5
CaO	8.5	8.4	7.3	5.2	5.1	5.0
Na ₂ O	3.0	3.2	3.5	3.3	3.4	3.7
K ₂ O	1.0	1.1	1.5	2.3	2.4	2.6
	100.0	100.1	100.0	100.1	100.2	100.3
<i>Mol. prop.</i>						
	$\frac{100 \text{ MgO}}{\text{MgO} + \text{FeO}_{\text{Total}}}$					
	47.7	45.3	37.8	41.0	38.9	35.9
<i>CIPW norm</i>						
Qz	10.7	12.5	19.2	15.5	16.4	17.6
Or	5.9	6.5	8.8	13.6	14.2	16.0
Ab	25.4	27.1	29.7	27.9	28.8	31.3
An	28.9	26.8	21.6	25.7	24.3	21.3
Diop	10.8	12.0	11.3	0.2	0.8	2.9
Hyp	11.3	7.8	0.5	14.8	13.1	8.7
Mt	4.3	4.8	4.8	0.4	0.4	0.4
Ilm	2.7	2.7	3.0	2.1	2.1	2.1
<i>Crystal residuum</i>						
SiO ₂		42.9	46.1		39.9	39.0
TiO ₂		0.8	1.0		0.9	1.0
Al ₂ O ₃		20.4	19.5		22.9	22.7
FeO		13.8	11.8		16.8	18.4
MnO		0.2	0.1		0.4	0.4
MgO		11.3	8.5		11.0	10.5
CaO		9.8	11.1		7.0	7.4
Na ₂ O		0.8	1.9		—	—
K ₂ O		—	—		—	—
		100.0	100.0		98.9	99.4
<i>Mol. prop.</i>						
	$\frac{100 \text{ MgO}}{\text{MgO} + \text{FeO}}$					
		59.3	56.2		53.9	50.4

^a Denotes compositions determined from analyses calculated in the manner described on p. 116.

18 kb contrasts strongly with the 27 and 36 kb trends as shown on these diagrams, and the latter trends closely approach those typical of the calc-alkaline series (see p. 107 and Fig. 13).

II. Experimental Investigation under Wet Conditions

Results

YODER and TILLEY (1962) conducted pioneering work on the crystallization of a number of natural basalt compositions under controlled water vapour pressure conditions from 0–10 kb. ($P_{H_2O} = P_{LOAD}$) using a gas apparatus. They demonstrated lowering of the liquidus of the compositions with increasing P_{H_2O} , together with an increase in the size of the field of crystallization of amphibole. There was also a pronounced increase in size of the partial melting interval (e.g. from 180 to 300° C in the high-alumina basalt as the P_{H_2O} increased from 0–10 kb).

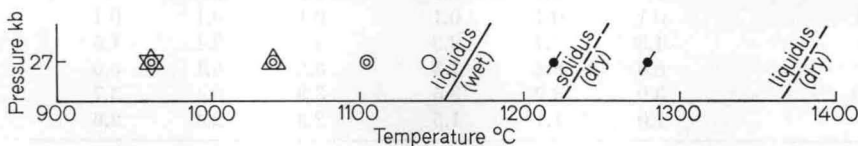


Fig. 12. Results of the experimental runs on the dacite composition under wet conditions. Key: ● Above liquidus. Phases co-existing with liquid: ○ clinopyroxene, ○ garnet, ▲ quartz, ▽ kyanite

An investigation of the phases crystallizing under wet conditions in the high-alumina quartz tholeiite, basaltic andesite, andesite and dacite compositions has been carried out. Because of the nature of the experimental procedure and the apparatus available (see p. 114), the P_{H_2O} is not closely controlled, but at 9–10 kb the pressure of water has resulted in lowering the liquidus of the compositions studied by about 200° C. The probable P_{H_2O} causing this effect would be from 2–5 kb P_{H_2O} ; the exact figure is not known.

The results of the wet runs are summarized in Tables 21 and 22, and Fig. 12.

a) Crystallization at 9–10 kb

In the high-alumina quartz tholeiite, clinopyroxene is the liquidus phase at about 1100° C and it is joined by orthopyroxene and amphibole at lower temperatures (e.g. 1040° C). Clinopyroxene becomes subordinate to amphibole at temperatures of about 960° C and less. Orthopyroxene is always only a minor phase. Plagioclase joins the ferromagnesian phases at about 920° C. Small, acicular, high relief and very strongly birefringent crystals occur in accessory amounts in most of the runs. Scanning of the needles using the electron microprobe indicates qualitatively that they are rich in iron and titanium. Identification is uncertain without quantitative analysis but the phase is probably pseudobrookite (as observed by YODER and TILLEY, 1962 in wet runs on basaltic compositions at similar pressures). A similar sequence of crystallization is observed in the basaltic andesite. Clinopyroxene, orthopyroxene and accessory pseudobrookite are the near-liquidus phases at 1020° C, joined by amphibole at 980° C, which becomes the major crystal phase by 960° C. These phases are joined by plagioclase at lower temperatures (e.g. 900° C). In contrast to these two compositions where plagioclase does not appear until temperatures are well below the liquidus for wet conditions, in the andesite composition under wet conditions at 10 kb clinopyroxene and plagioclase are the near-liquidus phases at 940° C. These phases are joined by garnet, amphibole, orthopyroxene and accessory pseudobrookite at 900° C.

b) Crystallization at 27 kb

Several runs have been conducted on the dacite composition, in order to determine the effect of the presence of water on the sequence of crystallization in the dacite composition at high pressure and also to obtain garnet crystals suitable for electron microprobe analysis. Garnet is the liquidus phase in the dacite at 1140° C and is joined at lower temperatures by clinopyroxene (1100° C), quartz (1040° C) and kyanite (960° C).

Analytical Data

a) Pyroxenes

Analyses of ortho- and clino-pyroxene from wet runs on the high-alumina quartz tholeiite composition are given in Table 23. The clinopyroxenes crystallizing from the wet runs are noteworthy for their high lime content compared with the lime content of the clinopyroxenes crystallizing from the higher temperature dry runs, indicating more solid-solution of orthopyroxene in clinopyroxene at the higher temperature. Alumina in tetrahedral co-ordination is also high in the clinopyroxene crystallizing from the wet runs and so the silica content is correspondingly low. Only two analyses of orthopyroxene crystallizing from wet runs at 9–10 kb have been obtained. These show a high alumina content in tetrahedral co-ordination, only slightly less than found in the co-existing clinopyroxene. The alumina content is higher, and the lime content lower than found in orthopyroxenes crystallized from basalts at similar pressures but under dry conditions and higher temperatures (D. H. GREEN and RINGWOOD, 1967b). The low lime content indicates lower solid-solution of clinopyroxene in orthopyroxene at lower temperatures.

b) Amphiboles (Table 24)

Five amphibole analyses are given in Table 24. Since water content could not be analyzed using the electron microprobe, the chemical formula has been calculated on an anhydrous basis, with 23 oxygens per formula unit. These amphiboles correspond to aluminous edenitic hornblendes with a significant alumina content in tetrahedral co-ordination and a low silica content. The titanium content is high. The $\frac{\text{Mg}}{\text{Mg} + \text{Fe}}$ ratio is significantly lower in the amphiboles than in co-existing pyroxenes.

c) Plagioclase (Table 25)

The plagioclase crystallizing well below the liquidus of the high-alumina quartz tholeiite under wet conditions is noteworthy for its high anorthite content, when compared with plagioclases crystallizing from a similar basalt under dry conditions (T. H. GREEN, 1968 in preparation).

Summary of the Most Significant Results

1. There is a large field of crystallization of amphibole, clinopyroxene and minor orthopyroxene at 9–10 kb in the basalt and basaltic andesite compositions i.e. crystallization of plagioclase is suppressed.
2. The amphiboles crystallizing are extremely sub-silicic (39.8–40.8% SiO₂).
3. The pyroxenes crystallizing have high alumina contents (7.5–10.6% Al₂O₃) and low silica contents (47.2–48.0% SiO₂).
4. The plagioclase crystallizing well below the liquidus in the basalt composition is quite calcic (An₆₆).
5. Plagioclase occurs near the liquidus in the andesite composition and is joined by garnet and amphibole at lower temperatures. Similar crystallization occurs in the rhyodacite, except that mica is present as well.
6. Increasing pressure results in increasing importance of garnet as a near-liquidus phase until at 18 kb in the rhyodacite (T. H. GREEN and RINGWOOD,

<i>Basaltic andesite</i>										
10	900	6	cpx	opx	amph		plag	glass	30	Abundant prismatic amphibole and plagioclase; minor stubby clinopyroxene and rare laths of orthopyroxene; amph, plag \gg cpx > opx
10	940	4	cpx	opx	amph			glass	60	Abundant prismatic amphibole; common stubby clinopyroxene; rare laths of orthopyroxene; amph > cpx \gg opx
10	960	4	cpx	opx ?	amph			psdb glass	70	As above except that accessory pseudobrookite present
10	980	4	cpx	opx	amph			psdb	80	Common stubby clinopyroxene, minor amphibole, rare laths of orthopyroxene and accessory pseudobrookite needles; cpx > amph > opx
10	1,020	4	cpx	opx				psdb	95	Minor stubby clinopyroxene and lath-like orthopyroxene; amphibole not identified; accessory pseudobrookite needles; opx > cpx
<i>Andesite</i>										
10	900	4 $\frac{1}{2}$	cpx	opx	amph	ga	plag	psdb glass	40	Abundant laths of plagioclase, minor euhedral garnet; rare amphibole, clino- and ortho-pyroxene; plag \gg cpx, ga > amph, opx
10	940	4	cpx				plag	glass	85	Large plagioclase laths common, rare stubby clinopyroxene; plag \gg cpx

1968) and at 27 kb in the dacite (this composition was not studied at 18 kb) garnet is the liquidus phase. The garnet appears to become enriched in grossular as well as pyrope with increasing pressure.

Interpretation of Results

As indicated previously (p. 114) the experimental procedure involving wet conditions was not ideal, and involved iron loss from some of the samples and uncertain water vapour pressures. In spite of these limitations the results on the crystallization of high-alumina quartz tholeiite at 9–10 kb ($P_{H_2O} < P_{LOAD}$) strongly support the hypothesis for the origin of the calo-alkaline series by the wet partial melting or fractional crystallization of basalt as outlined earlier (p. 112). Thus the large field of crystallization of sub-silicic amphibole together with subordinate clinopyroxene and minor orthopyroxene and possibly calcic plagioclase, provides an efficient mechanism for silica and alkali enrichment, and to a smaller extent alumina enrichment (before crystallization of calcic plagioclase begins).

Experimental runs on the dacite composition under wet conditions

been carried out to determine the liquidus phase in this composition at high pressures accompanied by water to grow garnets in the partial melting field large enough, and sufficiently free of inclusions, to allow for analysis. In this several exploratory runs under varying degrees of "wet" conditions were carried out before a final run was carried out without boron nitride sleeves and without sealing the sample capsule or drying the sample.

Water added (mgm)		Estimated % of glass	R.I. garnet (± 0.01)	Comments and estimated crystal phases present
—	qz cpx felds ga glass	20		Medium grained, garnet filled, qz, cpx \gg ga
—	qz cpx felds ga glass	50		Medium grained; pyroxene size; garnet large, inclusions; qz > cpx \gg ga \gg felds
<1	qz cpx felds ga glass	20		Similar to 1220°, 27 kbar
>1		glass	100	Above liquidus.
>1		glass	100	Above liquidus.
>1		ga glass	99	1.78 Rare, very large (50 μ) garnet, pale green color
>1	cpx ga glass	85	1.785	Common, large euhedral garnet, common aggregates of crystals.
>1	qz cpx ga glass	70	1.785	Common, large euhedral garnet, common stubby pyroxene; ga > cpx \gg qz.
>1	qz cpx ga ky glass	40		Abundant stubby pyroxene garnet crystals, minor kyanite; cpx > ga \gg qz, ky.
>1	qz cpx plag glass	?		Very fine grained, cpx smaller than rest; qz, plag >

Table 23. Electron microprobe analyses of clinopyroxenes and orthopyroxenes from selected wet runs

Composition	High-alumina quartz tholeiite											Dacite
Conditions of run	10 kb 920° C 7½ hrs Wet	10 kb 960° C 4 hrs Wet	9 kb 1,040° C 4 hrs Wet	9 kb 1,040° C 4 hrs Wet	10 kb 920° C 7½ hrs Wet	10 kb 960° C 4 hrs Wet	9 kb 1,040° C 4 hrs Wet	9 kb 1,040° C 4 hrs Wet	10 kb 960° C 4 hrs Wet	10 kb 940° C 6 hrs Wet	10 kb 960° C 4 hrs Wet	27 kb 1,100° C 60 mins Wet
	Runs conducted in platinum capsules,				Analyses adjusted for iron loss				Runs conducted in graphite capsules			ga ^b
Co-existing phases	amph ^b , opx plag ^b	amph ^b , opx	amph ^b , opx ^b	amph ^b , cpx ^b	amph ^b opx, plag ^b	amph ^b , opx	amph ^b , opx ^b	amph ^b cpx ^b	opx ^b ilm	amph ^b , opx, ilm	cpx ^b , ilm	
SiO ₂	47.2	48.0	47.3	47.5	46.7	47.5	46.8	46.3	51.7	52.0	49.4	50.0 ^a
TiO ₂	1.6	1.6	1.7	0.8	1.6	1.6	1.7	0.8	1.2	0.9	0.6	0.6
Al ₂ O ₃	10.0	10.6	8.6	7.5	9.9	10.5	8.5	7.3	9.2	11.3	8.4	15.0
FeO	7.0	6.1	5.8	11.8	9.0	7.9	7.6	15.4	6.4	8.3	11.1	6.2
MgO	11.6	11.9	14.9	26.6	10.5	10.9	13.9	24.5	13.6	13.8	27.9	9.0
CaO	21.6	18.7	20.1	1.7	21.4	18.5	19.9	1.7	19.7	19.8	1.4	15.9
Na ₂ O	0.7	0.7	0.6	—	0.7	0.7	0.6	—	0.1	0.2	—	2.7 ^a
$\frac{100 \text{ Mg}}{\text{Mg} + \text{Fe}}$	99.7	97.6	99.0	95.9	99.8	97.6	99.0	96.0	101.9	106.3	98.8	99.4
Formula 6 [0]	74.7	77.7	82.1	80.1	67.5	71.1	76.5	73.9	79.1	74.8	81.7	72.1
Si } ^z	1.7543	1.7922	1.7567	1.7722	1.7500	1.7888	1.7532	1.7588	1.8430	1.7904	1.7754	1.8156
Al } ^z	0.2457	0.2078	0.2433	0.2278	0.2500	0.2112	0.2468	0.2412	0.1570	0.2096	0.2246	0.1844
Al } ^{x+y}	0.1921	0.2585	0.1330	0.1018	0.1874	0.2586	0.1283	0.0857	0.2295	0.2490	0.1313	0.4577
Ti } ^{x+y}	0.0447	0.0448	0.0475	0.0224	0.0450	0.0453	0.0480	0.0228	0.0321	0.0234	0.0162	0.0164
Fe } ^{x+y}	0.2176	0.1905	0.1801	0.3682	0.2822	0.2490	0.2382	0.4892	0.1909	0.2386	0.3337	0.1884
Mg } ^{x+y}	0.6428	0.6626	0.8252	1.4800	0.5867	0.6122	0.7765	1.3878	0.7231	0.7086	1.4952	0.4874
Ca } ^{x+y}	0.8600	0.7479	0.7998	0.0679	0.8593	0.7465	0.7985	0.0692	0.7525	0.7303	0.0540	0.6185
Na } ^{x+y}	0.0505	0.0507	0.0433	—	0.0509	0.0512	0.0437	—	0.0068	0.0132	—	0.1899
z	2.00	2.00	2.00	2.00	2.00	2.00	2.00	2.00	2.00	2.00	2.00	2.00
x+y	2.01	1.96	2.03	2.04	2.01	1.96	2.03	2.05	1.94	1.96	2.03	1.96
AT. PROP.												
Mg	37.4	41.4	45.7	77.3	34.0	38.1	42.8	71.3	43.4	42.2	79.4	37.7
Fe	12.6	11.9	10.0	19.2	16.3	15.5	13.1	25.1	11.5	14.2	17.7	14.6
Ca	50.0	46.7	44.3	3.5	49.7	46.4	44.1	3.6	45.1	43.6	2.9	47.8

^a Denotes estimated content; reliable analytical figure not obtained. ^b Denotes co-existing phase analyzed.

Table 24. *Electron microprobe analyses of amphiboles from selected wet runs on the high-alumina quartz tholeiite composition*

Conditions of run	10 kb 920° C 7½ hrs Wet	10 kb 960° C 4 hrs Wet	9 kb 1,040° C 4 hrs Wet	9 kb 1,040° C 4 hrs Wet	10 kb 960° C 4 hrs Wet	10 kb 920° C 7½ hrs Wet	10 kb 940° C 6 hrs Wet	10 kb 920° C 5½ hrs Wet
	Runs conducted in platinum capsules			Analyses adjusted for iron loss to platinum capsules			Runs conducted in graphite capsules	
Co-existing phases	cpx ^a , opx, plag ^a	cpx ^a , opx	cpx ^a , opx ^a	cpx ^a , opx ^a	cpx ^a , opx	cpx ^a , opx, plag ^a	cpx ^a , opx, mt	cpx ^a , opx, mt
SiO ₂	40.5	40.8	39.8	39.3	40.2	39.9	40.0	40.2
TiO ₂	2.9	2.8	3.9	3.8	2.8	2.9	3.0	3.1
Al ₂ O ₃	15.8	14.4	15.8	15.6	14.2	15.6	14.8	15.4
FeO	10.0	8.2	7.6	9.8	10.6	12.6	9.4	9.8
MgO	13.1	14.9	14.9	13.7	13.6	11.6	12.9	12.1
CaO	12.4	11.7	12.0	11.8	11.5	12.2	11.6	11.8
Na ₂ O	2.5	2.7	2.9	2.9	2.7	2.5	2.0	1.8
K ₂ O	0.4	0.4	0.2	0.2	0.4	0.4	0.3	0.3
100 Mg Mg + Fe	97.6 70.3	95.9 76.4	97.1 77.8	97.1 71.4	96.0 69.6	97.7 62.1	94.0 71.0	94.5 68.8

Structural Formulae-calculated on "dry" basis of 23 [O] since H₂O content could not be determined

<i>z</i>	{Si	5.932	6.025	5.802	5.790	6.002	5.909	6.288	6.039
	{Al	2.068	1.975	2.198	2.210	1.998	2.091	1.712	1.961
	{Al	0.659	0.531	0.516	0.498	0.500	0.631	1.029	0.766
	{Ti	0.320	0.311	0.427	0.422	0.314	0.323	0.354	0.350
<i>y</i>	{Fe	1.209	1.013	0.927	1.208	1.324	1.561	1.236	1.231
	{Mg	2.862	3.281	3.239	3.011	3.029	2.561	3.024	2.710
	{Ca	1.945	1.851	1.874	1.862	1.840	1.936	1.954	1.899
<i>x</i>	{Na	0.709	0.861	0.820	0.829	0.781	0.717	0.610	0.524
	{K	0.074	0.075	0.037	0.037	0.075	0.075	0.060	0.058
<i>z</i>		8.00	8.00	8.00	8.00	8.00	8.00	8.00	8.00
<i>y</i>		5.05	5.14	5.11	5.14	5.17	5.08	5.64	5.06
<i>x</i>		2.73	2.79	2.73	2.73	2.70	2.79	2.62	2.48

^a Denotes co-existing phase analyzed.

Marked iron enrichment is prevented by the large degree of crystallization of amphibole with a relatively high Fe/Mg ratio, counteracting the effects of crystallization of pyroxenes with low Fe/Mg ratios. With increasing crystallization of plagioclase in extreme cases of fractionation the K/Na ratio of the fractionating liquids will increase.

The results obtained for the fractional crystallization at moderate pressure of high-alumina quartz tholeiite, basaltic andesite, andesite and rhyodacite under wet conditions are directly applicable to fractional crystallization of a hydrous

basaltic magma at 30–40 kms. depth (p. 112), and may also be applied in the reverse case of fractional melting of a basaltic composition at high pressure, where the sub-solidus assemblage consists mainly of amphibole, pyroxenes and plagioclase and possibly minor quartz and garnet. It is proposed that varying degrees of fractional melting or crystallization give rise to liquids comprising a typical calc-alkaline series. Thus for low degrees of melting the residuum will

Table 25. *Electron microprobe analysis of plagioclase from a wet run on the high-alumina quartz tholeiite composition*

Conditions of run	10 kb, 920° C, 7½ hrs
Co-existing phases	cpx ^b , opx, amph ^b
SiO ₂	52.9 ^a
Al ₂ O ₃	30.0
CaO	13.9
Na ₂ O	3.9
K ₂ O	0.1
	100.8
Mol prop.	
Or	0.6
Ab	33.4
An	66.0

^a Denotes calculated content.

^b Denotes co-existing phase analyzed.

wet conditions may give rise to dacitic or rhyodacitic liquids as the low melting fraction, rather than the andesitic low melting fraction obtained under dry conditions.

Calculation of Fractionation Trends

The experiments carried out under wet conditions for 4–8 hours in platinum capsules are accompanied by the loss of significant amounts of iron (e.g. an average loss of about 2.3% iron calculated as FeO — see Table 3) to the platinum capsule during the experiment. This results in the crystallization of phases possessing lower $\frac{100 \text{ Mg}}{\text{Mg} + \text{Fe}}$ ratios than would have occurred in runs without iron loss, and in turn, affects the calculated fractionation trend. However appropriate corrections may readily be applied to allow for this loss, and thus yield the true fractionation trend. Two independent methods have been used, leading to concordant results.

The average iron loss was determined by chemical analysis of two typical charges after the runs. Distribution factors for iron between the bulk composition (after the experiment) and crystallizing clinopyroxene, orthopyroxene and amphibole were determined using electron microprobe data, and the iron content of these three phases corresponding to the initial iron content of the bulk composition was obtained. The recalculated analyses of the phases were given in Tables 23

consist of amphibole, pyroxenes and plagioclase, and the liquid will be of dacitic or rhyodacitic composition with a high K/Na ratio. As the temperature increases the residuum becomes amphibole-pyroxene dominated and the liquid will be of andesitic composition, changing to basaltic andesite as the temperature rises further and melting of the mafic minerals of the residuum contributes significantly to the liquid. For $P_{\text{H}_2\text{O}} < P_{\text{LOAD}}$ temperatures necessary to produce calc-alkaline liquids would range from 900° C in the case of dacite and rhyodacite, to about 1000° C for basaltic andesite.

The crystallization of dacite at 27 kb under wet conditions where garnet not quartz is the liquidus phase, indicates that partial melting of eclogite at depths of 100–150 kms with in the earth, under

and 24. Corrections are comparatively small, e.g. clinopyroxene at 920° C is corrected from 7.0 to 9.0% FeO.

These corrections were verified subsequently by a series of wet runs in graphite capsules, preventing any iron loss (see Table 21 for details), and analyses of orthopyroxene, clinopyroxenes and amphibole from these runs have been obtained (Tables 23, 24). These analyses agree well, particularly the $\frac{100 \text{ Mg}}{\text{Mg} + \text{Fe}}$ values, with the corrected analyses of phases from platinum capsule runs. In making this comparison, phases from runs showing similar degrees of crystallization should be compared. Because of the difficulty in controlling water vapour pressure in these experiments, the runs in the graphite capsules show smaller degrees of crystallization than runs in the platinum capsules at the same temperature. Thus the run at 1040° C in platinum should be compared with the run at 940° C in graphite.

Using where necessary corrected analyses of phases as discussed above and their observed proportions, the fractionation trend of residual liquids obtained from the high-alumina quartz tholeiite under wet conditions has been calculated in Table 26. These liquids show marked silica and alkali enrichment, and also some alumina enrichment in the early stages. The $\frac{100 \text{ Mg}}{\text{Mg} + \text{Fe}}$ ratio obtained for varying degrees of crystallization follows that of the typical calc-alkaline trend, showing only minor enrichment relative to magnesium. The slight enrichment of iron relative to magnesium would have been decreased if the experiments had not been carried out under such reducing conditions, since under more oxidizing conditions a significant amount of iron in the trivalent state may be taken into the amphibole and pyroxene structures. For example amphiboles and pyroxenes from plutonic and effusive members of the calc-alkaline series contain a significant amount of ferric iron ($\frac{100 \text{ Fe}_2\text{O}_3}{\text{FeO} + \text{Fe}_2\text{O}_3}$) ranges from 15.7—48.6 for amphiboles and from 19.1—32.8 for clinopyroxenes; LARSEN *et al.*, 1936; AOKI, 1961; LIPMAN, 1964; DEER, 1938). The most significant feature of this experimental investigation at 9—10 kb under wet conditions where $P_{\text{H}_2\text{O}} < P_{\text{LOAD}}$, is that the amphiboles and pyroxenes are sub-silicic, so that extraction of these phases provides a very efficient means of enriching liquid fractionates in silica. Thus the residuum in equilibrium with a liquid of basaltic andesite composition will consist of approximately equal proportions of pyroxene and amphibole, while amphibole and subordinate pyroxene will form the residuum left after an andesite composition is extracted (the residuum will be approximately 45% by weight of the initial basalt). Finally amphibole, plagioclase, pyroxene and possibly minor

Note to Table 26

^a The orthopyroxene analysis obtained at 1,040°C, 9 kb has been used in calculations for other experimental runs since it could not be analyzed in these runs. Since only 2% of orthopyroxene is extracted, any variations in its composition will not seriously affect the compositions of the liquid fractionates or crystalline residua. Also 1% of ilmenite is extracted as part of the crystalline residua. This is because an accessory iron-titanium rich opaque mineral phase occurred in the experimental runs in graphite capsules where no iron loss took place. This phase could not be analyzed quantitatively and as a first approximation for these calculations was taken as ilmenite.

Table 26. *Calculated compositions of liquid fractionates and crystalline residua derived from the high-alumina quartz tholeiite at 9–10 kb under wet conditions^a*

Pressure		9 kb	10 kb	10 kb
Temperature		1,040° C	960° C	920° C
Nature and estimated % of crystals extracted	Initial liquid	18% cpx 5% amph 2% opx 1% ilm	18% cpx 25% amph 2% opx 1% ilm	18% cpx 32% amph 3% plag 2% opx 1% ilm
<i>Liquid fractionate</i>				
SiO ₂	52.9	55.9	59.7	64.5
TiO ₂	1.5	0.8	0.4	0.1
Al ₂ O ₃	16.9	19.4	20.2	19.9
Fe ₂ O ₃	0.3	0.4	0.5	0.7
FeO	7.9	7.2	5.8	3.7
MnO	0.2	0.3	0.3	0.4
MgO	7.0	4.4	2.1	2.0
CaO	10.0	7.8	6.7	3.9
Na ₂ O	2.7	3.3	3.4	3.6
K ₂ O	0.6	0.8	0.9	1.0
	100.0	100.3	100.0	99.8
Mol. prop.				
100 MgO				
MgO + FeO _{Total}	60.4	50.9	37.5	45.3
<i>CIPW norm</i>				
Qz		5.5	14.4	25.3
Or		4.8	5.4	5.9
Ab		27.9	28.8	30.5
An		35.7	33.2	19.3
Cor		—	1.4	5.8
Diop		2.4	—	—
Hyp		21.9	15.3	12.1
Mt		0.6	0.7	1.0
Ilm		1.5	0.8	0.2
<i>Crystal residuum</i>				
SiO ₂		44.8	43.0	42.7
TiO ₂		2.5	2.7	2.7
Al ₂ O ₃		9.7	12.3	14.2
FeO		9.1	10.1	11.2
MgO		14.6	12.9	11.0
CaO		16.6	13.8	14.8
Na ₂ O		1.0	1.8	1.9
K ₂ O		0.04	0.2	0.2
		98.34	96.8	98.7
Mol. prop.				
100 MgO				
MgO + FeO		74.2	69.5	63.7

Table 27. *Calculated compositions of liquid fractionates and crystalline residua derived from the dacite composition under wet conditions at 27 kb*

Temperature		1,140° C	1,100° C
Nature and estimated % of crystals	Initial liquid	1% ga	9% ga 6% cpx
<i>Liquid fractionate</i>			
SiO ₂	65.0	65.3 ^a	68.8 ^a
TiO ₂	0.7	0.7	0.6
Al ₂ O ₃	16.1	16.0	15.6
Fe ₂ O ₃	1.4	1.4	1.6
FeO	3.5	3.3	1.5
MnO	0.1	0.1	0.1
MgO	1.8	1.7	0.6
CaO	5.0	5.0	3.8
Na ₂ O	3.6	3.6	4.1
K ₂ O	2.1	2.1	2.5
Mol. prop.	99.3	99.2	99.2
100 MgO			
MgO + FeO _{Total}	40.3	39.9	26.7
<i>CIPW norm</i>			
Qz	21.7	22.0	26.5
Or	13.0	12.4	14.8
Ab	30.5	30.5	34.6
An	21.5	21.3	16.8
Diop	2.3	2.9	1.7
Hyp	7.7	6.8	1.3
Mt	2.0	2.0	2.3
Ilm	1.3	1.3	1.1
<i>Crystal residuum</i>			
SiO ₂		39.4	43.2
TiO ₂		1.5	1.3
Al ₂ O ₃		21.4	18.8
FeO		19.8	15.1
MnO		0.3	0.2
MgO		8.9	8.4
CaO		8.8	12.1
Na ₂ O		—	1.0
K ₂ O		—	—
Mol prop.		100.1	100.1
100 MgO			
Mg + FeO		44.5	49.8

^a Denotes compositions determined from analyses calculated in the manner described on p. 114.

garnet will constitute the residuum when dacitic or rhyodacitic liquids are extracted.

The alumina content of the liquids is high compared with the content normally found in members of the calc-alkaline series. This is attributed to the fact that the experiments have been conducted on a high-alumina basaltic composition. If a basalt with an alumina content of about 14% had been used then the alu-

mina enrichment in the early stages, caused by the separation of pyroxenes and amphibole, would probably have resulted in compositions corresponding to basaltic andesite and andesite with alumina contents of 16–17%. Continued fractionation would involve plagioclase so that the alumina content of the liquid would then decrease. However it is significant to note that although some alumina enrichment occurs in the early stages of fractionation, derivation of liquids of highly aluminous compositions such as anorthosite or gabbroic anorthosite by the fractionation of basalt under wet conditions is not likely (c.f. suggestion of YODER and TILLEY, 1962; YODER, 1966; BUDDINGTON, 1961). The liquids obtained are too enriched in silica and depleted in lime to correspond to gabbroic anorthosite. Also alumina enrichment is not sufficiently high before crystallization of plagioclase begins. The problem of the derivation of anorthositic compositions is dealt with in greater detail elsewhere (T. H. GREEN, 1966, 1967b).

Comparison of Experimental Fractionation Trends with Natural Calc-Alkaline Trends

The general fractionation trends under dry conditions for the two basalts, basaltic andesite and andesite compositions at 27–36 kb are plotted in Fig. 13. For

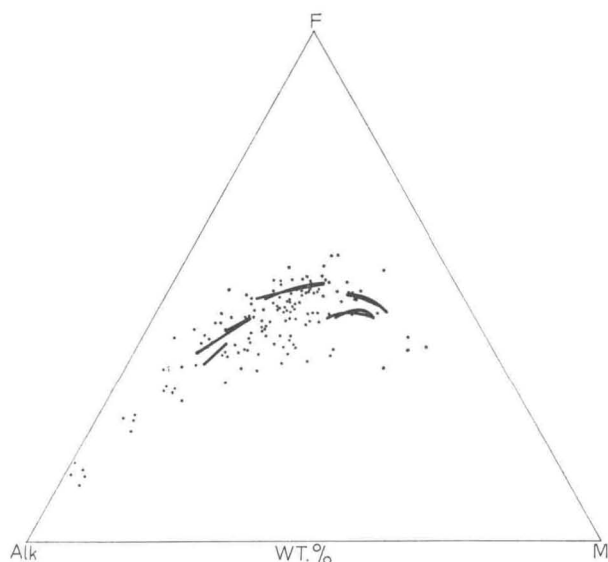


Fig. 13. FMA plot for the Aleutian Islands calc-alkaline province. The experimentally determined fractionation trends at 27–36 kb are superimposed on this plot as solid lines for comparison between the natural and experimental fractionation trends

comparison, a plot of analyses of calc-alkaline rocks from the Aleutian island arc calc-alkaline province is also given. The similarity of the trends is apparent. Minor iron enrichment relative to magnesium occurs in the more basic compositions, but there is no marked iron enrichment as characterized by tholeiitic series (e.g. SKAERGAARD, WAGER, 1960; THINGMULI, CARMICHAEL, 1964; KUNO's pigeonitic series of Japan, KUNO, 1965). The fractionation trends observed

experimentally at 18 kb (Fig. 9) do show marked iron enrichment, and at this pressure (and lower pressures as well, since similar phases dominate the crystallization under dry conditions from 0—18 kb) the trends are similar to the typical tholeiitic fractionation trends.

A feature frequently exhibited by basalt to andesite members of the natural calc-alkaline series is the uniform increase in soda and potash contents with increasing silica content of the rocks (also the K_2O/Na_2O ratio increases uniformly but stays less than unity) until the silica content reaches about 60—65%. For more acid members of the series, the potash content continues to increase but soda begins to decrease, and consequently the K_2O/Na_2O ratio increases sharply to greater than unity. It is explained by the present experimental work since fractionation trends for members of the suite ranging from basalt to andesite are dominated by pyroxene and garnet (model I — dry melting at 27—36 kb) or by pyroxene and amphibole (model II wet melting at about 10 kb). Of these phases garnet contains no detectable soda or potash, pyroxenes contain minor soda (e.g. 0.6—3.0%) but no detectable potash, and amphibole contains minor soda (e.g. 2.0—2.9%) and subordinate potash (e.g. 0.2—0.4%). Thus extraction of garnet + pyroxene or amphibole + pyroxene results in an increase in both soda and potash in the liquid fractionates, together with a slight increase in the K_2O/Na_2O ratio (due to the small but significant content of Na_2O and the absence of K_2O in the pyroxenes).

However compositions more acid than andesite may only be derived under dry conditions in model I by fractionation at crustal pressures. At these pressures the crystallization is dominated by plagioclase with the result that the more acid liquids obtained are depleted in soda relative to potash. Similarly in model II in compositions more acid than andesite, crystallization becomes dominated by plagioclase. Thus a sharp increase in K_2O/Na_2O ratio in acid members of the calc-alkaline series result. Alternatively in model I if wet conditions ($P_{H_2O} < P_{LOAD}$) prevail at 27—36 kb more silica-rich compositions than andesite such as dacite or granodiorite may be derived, but in these cases the K_2O/Na_2O ratio will remain less than unity, unless subsequent fractional crystallization occurs at crustal pressures. The silica-rich but potash-poor dacites of Saipan, Marianas Islands (SCHMIDT, 1957) with low K_2O/Na_2O ratios may have originated by wet partial melting at mantle depths.

Geological Evidence

a) Garnet Phenocrysts in Calc-Alkaline Rocks

Almandine-rich garnet phenocrysts have been recorded in rocks of the calc-alkaline suite from Australia (EDWARDS, 1936; RINGWOOD, 1955), New Zealand (COX, 1926), Japan (MIYASHIRO, 1955), England (OLIVER, 1956), and Russia (MAKAROV and SUPRYCHEV, 1964). They are most common in dacites, rhyodacites and granodiorites, but may also occur in andesites and rhyolites. MIYASHIRO (1955) emphasized the compositional differences between garnets occurring as phenocrysts in calc-alkaline lavas and plutonic rocks (almandine-rich with some pyrope, spessartine poor), and those occurring either in cavities in calc-alkaline lavas, or in pegmatites associated with calc-alkaline plutonic rocks (almandine-spessartine-rich, pyrope poor). EDWARDS (1936) and OLIVER (1956) concluded

that the phenocrystic garnets initially crystallized directly from the magma under equilibrium conditions at an early stage of crystallization, and later became unstable in their subsequent environment.

The experimental work described in this paper has shown that almandine-rich garnets occur on and near the liquidus in calc-alkaline rocks at high pressure. These results, when considered in relation to the phenocrystic habit of the natural almandine garnets found in calc-alkaline rocks, suggest that the garnets formed from the calc-alkaline magma at an early stage of crystallization at great depth within the earth. These garnets subsequently react to a low pressure assemblage (e.g. cordierite-hypersthene) at high levels in the crust.

An investigation of the origin of these garnets has been described in an accompanying paper (T. H. GREEN and RINGWOOD, 1968). In this study almandine-rich garnets were crystallized on or near the liquidus in a natural rhyodacite composition at pressures of > 9 kb. From a comparison of the composition of the near-liquidus garnets obtained experimentally with the composition of a large number of natural garnet phenocrysts from calc-alkaline rocks of Victoria, Australia, it was concluded that the garnet phenocrysts provide relict evidence for the early crystallization of calc-alkaline magmas at depth, and consequently support the models involving the origin of the calc-alkaline series in the upper mantle or lower crust.

b) Resorbed Quartz Phenocrysts in Calc-Alkaline Rocks

As mentioned on p. 108 quartz phenocrysts showing varying degrees of resorption commonly occur in the acid members of the calc-alkaline series. This resorption has been attributed to fluctuation in water vapour pressure in the partially crystallized magma (EWART, 1965). This alters the position of the quartz-feldspar minimum (TUTTLE and BOWEN, 1958) and may cause the resorption of quartz. However in such a mechanism the release of water vapour pressure would result in a rise in liquidus temperature and consequently an increase in crystallization. This would be the major effect — any shift in the eutectic causing feldspar instead of quartz to crystallize (and hence causing resorption of quartz) would be a second order feature. The present experimental work indicates that resorption may also be due to change in load pressure. Thus at high pressure under dry conditions, quartz is the liquidus phase in the rhyodacite and dacite compositions, but at low pressure quartz is replaced by feldspar as the liquidus phase. Hence a magma rising from depth may contain early crystallized quartz phenocrysts which when carried into a low pressure environment are no longer in equilibrium with the melt and so undergo resorption. The comparative abundance of quartz phenocrysts in the acid calc-alkaline magmas and the rarity of garnet may be explained by the ease of transport of quartz phenocrysts compared with garnet, due to the small density difference between quartz and the acid magma, compared with the large density difference between garnet and the magma.

c) Trace Element Distribution and Isotope Ratios in the Calc-Alkaline Suite

At present there is a scarcity of systematic data on the trace element distribution and the isotope ratios of the various rock types comprising the calc-alkaline suite in a particular province. NOCKOLDS and ALLEN (1953) have carried out an investigation of the trace element distribution in members of the calc-alkaline

provinces of north-western North America, the Southern Californian batholiths, Lesser Antilles, and the Scottish Caledonian. TAYLOR and WHITE (1966) report the trace element content of a number of andesites from Japan and New Zealand.

In the two stage process proposed for the origin of the calc-alkaline suite, the trace element distribution will be governed by the initial distribution in the basalt pile developed as a first stage in the process, and then by the nature of the partial melting processes operating in the second stage, and finally by the subsequent rise of the magma to the earth's surface. D. H. GREEN and RINGWOOD (1967) indicated that simple crystal fractionation in a closed system could not explain the minor element chemistry of basalts. They outlined and discussed processes of wall-rock reaction and wall-rock contamination which may operate to modify the trace element distribution observed in basalts, and which may produce a considerable variation in the distribution of the trace elements and in the isotope ratios.

Similar arguments apply to the derivation of the calc-alkaline suite, but in this case the final result may be extremely variable from one calc-alkaline province to another, because of the potential duplicated interplay of processes of wall-rock reaction and contamination during the two stage genesis of the calc-alkaline series. Also there may be extensive reaction and contamination of the calc-alkaline magma where it intrudes through great thicknesses of sediments in active orogenic areas. Thus it may be very hard to determine patterns of distribution of minor elements which are characteristic of the calc-alkaline series in general.

An increasing amount of data on initial strontium isotope ratios found for the calc-alkaline series indicates that the ratio $\text{Sr}^{87}/\text{Sr}^{86}$ characteristically falls in the range from about 0.704—0.708 (HURLEY *et al.*, 1965; EWART and STIPP, 1967). This is significantly lower than expected for ratios obtained in calc-alkali rocks derived from magma generation by anatexis processes involving old crustal rocks. It is also significantly higher than the ratio typical of oceanic tholeiites, and believed to represent the mantle $\text{Sr}^{87}/\text{Sr}^{86}$ ratio, at least in oceanic areas (ENGEL, ENGEL and HAVENS, 1964). However the above range of $\text{Sr}^{87}/\text{Sr}^{86}$ for the calc-alkaline series overlaps with the range of ratios found for some continental tholeiites (GAST, 1960; FAURE and HURLEY, 1963).

The two stage models for the origin of the calc-alkaline series proposed in this work can explain the relatively low values for the initial strontium isotope ratios, since melting of a basalt pile with low strontium isotope ratios characteristic of basaltic rocks would give rise to derivative magmas with correspondingly low ratios. Conversely because of the possible variation in the $\text{Sr}^{87}/\text{Sr}^{86}$ ratio of the initial basalt pile, calc-alkaline rocks derived from such piles, according to either of the two models outlined, may have moderately high initial strontium isotope ratios (e.g. up to 0.708). Thus contamination with material enriched in radiogenic strontium is not essential to produce isotope ratios of these values in the calc-alkaline series.

From a study of the lead isotopes from western and midwestern United States, DOE (1967) suggested that one possible explanation of the data was that the rocks were derived by partial melting of basaltic-gabbroic parent material, possibly in the mantle in the western coastal regions and in the lower crust in the mid-western interior regions. The data preclude derivation of the calc-alkaline rocks

by partial or complete melting of older granitic rocks. Thus these conclusions support the hypotheses for the origin of the calc-alkaline igneous rock series presented in this paper.

Summary

The experimental work supports three possible models for the origin of the calc-alkaline suite. These models have been outlined in the introductory sections of this paper. In two of the models the calc-alkaline series forms as a result of a two-stage magmatic process. In the first stage, fractional melting of the pyrolite mantle produces undersaturated basaltic magma which rises to higher levels and following fractionation of this magma at depths of less than 15 kms, large piles of basalt with an overall quartz-normative composition will be formed. Likely crustal areas where such piles may develop include continental margins, oceanic rift systems, island arcs and some oceanic rises (RINGWOOD and D. H. GREEN, 1966). If the geotherms in the area where the basalt pile has developed drop after the basaltic volcanism has ceased, and the basalt pile remains dry, then it may eventually transform to eclogite (RINGWOOD and D. H. GREEN, 1966) and sink back into the mantle. The mineralogy of the sinking eclogite will consist of chiefly garnet-clinopyroxene-quartz. In the second stage of the two stage process at depths of approximately 100—150 kms where the temperatures are sufficiently high, partial melting of the eclogite will take place, giving rise to members of the calc-alkaline suite. If the melting takes place under dry conditions basaltic andesite or andesite (plutonic diorite or quartz diorite) will be obtained, or if wet melting takes place, dacite or rhyodacite (plutonic granodiorite or adamellite) will be produced. The initial overall composition of the basaltic pile and the temperature and depth at which partial melting of the eclogite occurs, will be important factors in governing the composition of the calc-alkaline magmas obtained. However, additional processes such as varying degrees of crystallization of the magma during its upwards progress will also operate, causing variation in composition of the final lava flow or pluton. For instance some dacite and rhyolite magmas may be derived from andesite by fractional crystallization at pressures corresponding to those deep within the crust, leaving a residuum of plagioclase and subordinate pyroxene (gabbroic anorthosite — T. H. GREEN, 1967b); the low melting liquid resulting will vary from dacite to rhyolite depending on the degree of fractionation. This mechanism is probably significant in provinces where the K_2O/Na_2O ratio is greater than unity in the more acid members of the calc-alkaline suite and is similar to the plagioclase effect proposed by BOWEN (1928).

Alternatively in the second model proposed, access of water to the basalt pile developed in continental margin or island arc areas results in formation of amphibolite in the lower parts of the pile. The water content of such an amphibolite may be of the order of 1%. Subsequent heating of this amphibolite, due to renewed or continued volcanic activity from the mantle, may result in partial melting taking place. The pressures at which partial melting takes place may be as high as 10 kb, corresponding to the base of the crust, but water vapour pressure is likely to be less than load pressure and the magmas produced will not be saturated in water, since insufficient water occurred in the parent amphibolite. The residual phases from such melting will consist mainly of amphibole and clinopyroxene and subordinate orthopyroxene, calcic plagioclase and possibly garnet,

depending on the degree of partial melting. As in the first model, the initial overall composition of the basalt pile and the temperature and depth at which wet partial melting of the basalt occurs, will be important factors determining the composition of the derived calc-alkaline magmas. Similarly the rate of progress of the magma to the surface and the degree of crystallization during this movement will cause variation in composition of the final lava flow or pluton. The fact that the melting has taken place under conditions of $P_{H_2O} < P_{LOAD}$ means that decrease in pressure due to upward movement of the magma will not result in sudden crystallization due to the raising of the liquidus consistent with the lower P_{H_2O} . This would be the case if $P_{H_2O} = P_{LOAD}$ in the magma unless the magma was in a superheated condition.

The residuum left after partial melting of the amphibolite may remain as a lower crust of amphibolite or alternatively it may subsequently transform to eclogite, if most of the water has been driven off and if the temperature decreases. The eclogite will then sink into the mantle (cf. RINGWOOD and D. H. GREEN, 1966). This will solve any room problem regarding the presence of a large crystalline residuum remaining after the partial melting process.

A third model for the origin of the calc-alkaline series involves the fractional crystallization of a hydrous basalt magma at 30–40 kms depth. The basalt magma is derived by partial melting of the mantle (cf. D. H. GREEN and RINGWOOD, 1967b). Access of water to the magma may have resulted from contamination with hydrated rocks introduced into the mantle by a sinking limb of a convection cell, as in the hypothesis of "sea-floor spreading" (HESS, 1962). This, in turn, might also explain the association of calc-alkaline rocks with a particular tectonic environment.

These models provide a mechanism for adding sialic material to the crust from the mantle as a result of a two stage process. Features of the calc-alkaline series which may be explained by these models include:

- (i) The characteristic Fe/Mg fractionation trend, which shows only slight iron enrichment relative to magnesium with increasing acidity. This is attributed to the presence of relatively iron-rich mafic phases (garnet or amphibole — see Tables 11, 24) in the residuum left after fractional melting or crystallization.
- (ii) The sequence and relative volumes of the different rock types. This is governed by the composition of the initial basalt pile, the depth and degree of partial melting or fractional crystallization and whether it is dry or wet melting and finally the progress of the liquid to its final site of crystallization.
- (iii) Low initial Sr^{87}/Sr^{86} ratios of members of both the extrusive and plutonic calc-alkaline series, due to their derivation from basaltic material with a low initial Sr^{87}/Sr^{86} ratio.
- (iv) Presence of almandine-rich garnets of magmatic origin in the more acid members of the calc-alkaline series. These may have formed at lower crustal or upper mantle pressures.
- (v) Presence of resorbed quartz phenocrysts in dacites and rhyodacites. These may have crystallized at depth and later became out of equilibrium when carried in the magma to a low pressure environment.

In addition, the models described provide a highly efficient way of deriving acidic compositions from a basic parent, by separation of silica-poor garnet and aluminous pyroxene phases (model I) or silica-poor amphibole and aluminous

pyroxene phases (models II and III). Thus, during fractional melting or crystallization of a basaltic composition at upper mantle (model I) or lower crustal (models II and III) pressures, the mass ratio of residual phases to andesitic magma produced is approximately unity. In contrast, in models involving fractional crystallization of low pressure phases (plagioclase, pyroxene and olivine) from a basalt, the ratio of crystalline material to magma would be two or more, even under idealized conditions. There is no room problem in either model, since in both cases the residuum may sink into the mantle, and would rarely be available for sampling by geological processes.

Acknowledgements. We wish to thank Dr. D. H. GREEN for critically reading an early draft of this paper.

References

- AKIMOTO, S.: Thermo-magnetic study of ferromagnetic minerals contained in igneous rocks. *J. Geomag. Geoelect.* **6**, 1—14 (1954).
- Magnetic properties of ferromagnetic minerals contained in igneous rocks. *Jap. J. Geophys.* **1**, 1—31 (1955).
- ANDERSON, C. A.: Volcanoes of the Medicine Lake Highland, California. *Calif. Univ., Dept. Geol. Sci. Bull.* **25**, 347—422 (1941).
- AOKI, K.: On hornblende from Ammadaki, Iki Islands, Northern Kyushu, Japan. *J. Japan. Assoc. Mineralogists, Petrologists, Geologists* **45**, 115—119 (1961).
- BOWEN, N. L.: The evolution of igneous rocks. Princeton: Univ. Press 1928.
- BOYD, F. R., and J. L. ENGLAND: Apparatus for phase-equilibrium measurements at pressures up to 50 kb and temperatures up to 1750° C. *J. Geophys. Research* **65**, 741—748 (1960).
- Effect of pressure on the melting point of diopside, $\text{CaMgSi}_2\text{O}_6$ and albite $\text{NaAlSi}_3\text{O}_8$ in the range up to 50 kb. *J. Geophys. Research* **68**, 311—323 (1963).
- BRANCH, C. D.: Genesis of magma for acid calc-alkaline volcano-plutonic formations. *Tectonophysics* **4**, 83—100 (1967).
- BUDDINGTON, A. F.: The origin of anorthosite re-evaluated. *Records Geol. Survey India* **86**, 421—432 (1961).
- BYERS jr., F. M.: Petrology of three volcanic suites, Umnak and Bogoslof Islands, Aleutian Islands, Alaska. *Bull. Geol. Soc.* **72**, 93—128 (1961).
- CARMICHAEL, I. S. E.: The petrology of Thingmuli, a Tertiary volcano in eastern Iceland. *J. Petrology* **5**, 435—460 (1964).
- The iron-titanium oxides of salic volcanic rocks and their associated ferromagnesian silicates. *Contr. Mineral. and Petrol.* **14**, 36—64 (1967).
- CLARK, R. H.: Petrology of the volcanic rocks of Tongariro sub-division. *Bull. New Zealand Geol. Surv.* **40**, Appendix 2, 107—123 (1960).
- COATS, R. R.: Magmatic differentiation in Tertiary and Quaternary volcanic rocks from Adak and Kanaga Islands, Aleutian Islands, Alaska. *Bull. Geol. Soc. Amer.* **63**, 485—514 (1952).
- Magma type and crustal structure in the Aleutian Arc, in *Crust of the Pacific Basin*. *Geophys. Mon.* **6**, 92—109 (1962).
- Geologic reconnaissance of Semisopochnoi Island, Western Aleutian Islands, Alaska. *U.S. Geol. Survey, Bull.* **1028-0** (1959).
- COOMBS, H. A.: Mt. Baker, a Cascade volcano. *Bull. Geol. Soc. Am.* **50**, 1493—1510 (1939).
- COX, P. T.: Geology of the Rakaia gorge district. *Trans. Proc. New Zealand Inst.* **56**, 91—111 (1926).
- DALY, R. A.: *Igneous rocks and the depths of the earth*. New York: McGraw-Hill Book Co. Inc. 1933.
- DEER, W. A.: The composition and paragenesis of the hornblendes of the Glen Tilt Complex, Perthshire. *Mineral. Mag.* **25**, 56—74 (1938).
- DICKINSON, W. R.: Circum-Pacific andesite types. *Abst. Trans. Am. Geophys. Union* **48**, 253 (1967).

- DOE, B. D.: The bearing of lead isotopes on the source of granitic magma. *J. Petrology* 8, 51—83 (1967).
- DREWES, H., G. D. FRASER, G. L. SNYDER, and H. F. BARNETT jr.: Geology of Unalaska Island and adjacent insular shelf, Aleutian Islands, Alaska. U.S. Geol. Surv., Bull. 1028-S (1961).
- EDWARDS, A. B.: On the occurrence of almandine garnets in some Devonian igneous rocks of Victoria. *Proc. Roy. Soc. Victoria* 49, 40—50 (1936).
- ENGEL, A. E. J.: Geologic evolution of North America. *Science* 140, 143—152 (1963).
- C. G. ENGEL and R. G. HAVENS: Chemical characteristics of oceanic basalts and the upper mantle. *Bull. Geol. Soc. Am.* 76, 719—734 (1965).
- ENGEL, C. G., R. L. FISHER and A. E. J. ENGEL: Igneous rocks of the Indian Ocean floor. *Science* 150, 605—610 (1965).
- EWART, A.: Mineralogy and petrology of the Whakamaru Ignimbrite in the Maraetai area of the Taupo Volcanic Zone, New Zealand. *New Zealand J. Geol. Geophys.* 8, 611—677 (1965).
- , and J. J. STIPP: Origin of the volcanic rocks of the Central North Island, New Zealand, as indicated by a study of Sr^{87}/Sr^{86} ratios and Sr, Rb, K, U and Th abundances. *Geochim. et Cosmochim. Acta* (1967, in press).
- FAURE, G., and P. M. HURLEY: The isotopic composition of strontium in oceanic and continental basalts: application to the origin of igneous rocks. *J. Petrology* 4, 31—50 (1963).
- GAST, P. W.: Limitations on the composition of the upper mantle. *J. Geophys. Research* 65, 1287—1297 (1960).
- GORSHKOV, G. S.: Petrochemical features of volcanism in relation to the types of the earth's crust, in "Crust of the Pacific Basin". *Geophys. Mon.* 6, 110—115 (1962).
- GREEN, D. H., and I. B. LAMBERT: Experimental crystallization of anhydrous granite at high pressures and temperatures. *J. Geophys. Research* 70, 5259—5268 (1965).
- —, and A. E. RINGWOOD: An experimental investigation of the gabbro to eclogite transformation and its petrological applications. *Geochim. et Cosmochim. Acta* 31, 767—833 (1967a).
- — — The genesis of basalt magmas. *Contr. Mineral. and Petrol.* 15, 103—190 (1967b).
- GREEN, T. H.: High pressure experiments on the genesis of anorthosites, in "Petrology of the upper mantle". *Aust. Nat. Univ. Dept. Geophys. and Geochem., Publ.* 444 (1966).
- High pressure experimental investigations on the origin of high-alumina basalt, andesite and anorthosite, Unpubl. Ph. D. Thesis, Aust. Nat. Univ. (1967a).
- Experimental fractional crystallization of quartz diorite and its application to the problem of anorthosite origin. In: *Symposium on "Origin of Anorthosite"* (ed. Y. ISACHSEN) (in press, 1967b).
- High pressure experimental study of the origin of anorthosite. In preparation (1968).
- D. H. GREEN and A. E. RINGWOOD: The origin of high-alumina basalts and their relationships to quartz tholeiites and alkali basalts. *Earth and Planetary Sci. Letters* 2, 41—51 (1967).
- , and A. E. RINGWOOD: Origin of the calc-alkaline igneous rock suite. *Earth and Planetary Sci. Letters* 1, 307—316 (1966).
- — Origin of garnet phenocrysts in calc-alkaline rocks. *Contr. Mineral. and Petrol.* 18, 163—174 (1968).
- —, and A. MAJOR: Friction effects and pressure calibration in a piston-cylinder apparatus at high pressure and temperature. *J. Geophys. Research* 71, 3589—3594 (1966).
- HAMILTON, W.: Origin of high-alumina basalt, andesite and dacite magmas. *Science* 146, 635—637 (1964).
- HESS, H. H.: The Stillwater Igneous Complex, Montana. *Geol. Soc. Am. Mem.* 80 (1960).
- HOLMES, A.: The origin of igneous rocks. *Geol. Mag.* 69, 543—558 (1932).
- HURLEY, P. M., P. C. BATEMAN, H. W. FAIRBAIRN, and W. H. PRINSON jr.: Investigation of initial Sr^{87}/Sr^{86} ratios of the Sierra Nevada plutonic province. *Bull. Geol. Soc. Am.* 76, 165—174 (1965).
- IRVINE, T. N.: Origin of the ultramafic complex at Duke Island, southeast Alaska. *Min. Soc. Am., Spec. Pap.* 1, 36—45 (1963).
- JOPLIN, G. A.: A petrography of Australian igneous rocks. Sydney: Angus and Robertson 1965.

- KOSMINSKAYA, I. P., S. M. ZVEREV, P. S. VEITSMAN, YU. V. TULINA and R. M. KRAKSHINA: Basic features of the crustal structure of the Sea of Okhotsk and the Kurile-Kamchatka zone of the Pacific Ocean from deep seismic sounding data. *Bull. Acad. Sci. U.S.S.R., Geophys. Ser. (Eng. Transl.)*, 11—27 (1963).
- KUNO, H.: Petrology of the Hakone Volcano and adjacent areas, Japan. *Bull. Geol. Soc. Am.* **61**, 957—1020 (1950).
- High-alumina basalt. *J. Petrology* **1**, 121—145 (1960).
- Some problems of calc-alkali rock series, Japan. *J. Japan. Assoc. Mineralogists, Petrologists Econ. Geologists* **53**, 131—142 (1965).
- LARSEN, E. S., and W. DRAISIN: Composition of the minerals in the rocks of the Southern Californian Batholith, Rept. 18th Sess. Internat. Geol. Congr. 1948, **2**, 66—79 (1948).
- J. IRVING, and F. A. GONYER: Petrologic results of a study of the minerals from the Tertiary volcanic rocks of the San Juan region, Colorado. *Am. Mineralogist* **21**, 679—701 (1936).
- — — Petrologic results of a study of the minerals from the Tertiary volcanic rocks of the San Juan region, Colorado. *Am. Mineralogist* **23**, 417—429 (1938).
- LIDIAK, E. G.: Petrology of andesitic, spilitic and keratophyric flow rock, north-central Puerto Rico. *Bull. Geol. Soc.* **76**, 57—88 (1965).
- LIPMAN, P. W.: Mineralogy and paragenesis of amphibole from Gibson Peak Pluton, Northern California. *Am. Mineralogist* **49**, 1321—1330 (1964).
- MACDONALD, G. A., and T. KATSURA: Chemical composition of Hawaiian lavas. *J. Petrology* **5**, 82—133 (1964).
- — — Eruption of Lassen Peak, Cascade Range, California in 1915: example of mixed magmas. *Bull. Geol. Soc. Am.* **76**, 475—482 (1965).
- MAKAROV, N. N., and V. A. SUPRYCHEV: Xenogenic garnet (pyrope-almandine) from volcanic rocks of the Crimea. *Doklady Akad. Nauk S.S.R. (Eng. Transl.)* **157**, 64—67 (1964).
- MIYASHIRO, A.: Pyrope garnets in volcanic rocks. *J. Geol. Soc. Japan* **61**, 463—470 (1955).
- NOCKOLDS, S. R.: The production of normal rock types by contamination and their bearing on petrogenesis. *Geol. Mag.* **71**, 31—39 (1934).
- , and R. ALLEN: The geochemistry of some igneous rock series. *Geochim. et Cosmochim. Acta* **4**, 105—142 (1953).
- O'HARA, M. J.: Melting of garnet peridotite at 30 kilobars. *Carnegie Inst. Wash. Year Book* **62**, 71—76 (1963a).
- Melting of bimineraleclogite at 30 kilobars. *Carnegie Inst. Wash. Year Book* **62**, 76—77 (1963b).
- Primary magmas and the origin of basalts. *Scot. J. Geol.* **1**, 19—40 (1965).
- OLIVER, R. L.: The origin of garnets in the Borrowdale Volcanic Series and associated rocks, English Lake District. *Geol. Mag.* **93**, 121—139 (1956).
- OSBORN, E. F.: Role of oxygen pressure in the crystallization and differentiation of basaltic magma. *Am. J. Sci.* **257**, 609—647 (1959).
- Reaction series for sub-alkaline igneous rocks based on different oxygen pressure conditions. *Am. Mineralogist* **47**, 211—226 (1962).
- POLDERVAART, A.: Three methods of graphic representation of chemical analyses of igneous rocks. *Trans. Roy. Soc. S. Africa* **32**, 177—188 (1949).
- , and W. ELSTON: The calc-alkaline series and the trend of fractional crystallization of basaltic magma. A new approach at graphical representation. *J. Geol.* **62**, 150—162 (1954).
- RINGWOOD, A. E.: Geology of the Deddick-Wulgulmerang area, East Gippsland. *Proc. Roy. Soc. Victoria* **67**, 19—66 (1955).
- The chemical composition and origin of the earth. In: *Advances in Earth Sciences* (ed. P. M. HURLEY), pp. 287—356. Cambridge, Mass: M.I.T. Press 1966.
- , and D. H. GREEN: An experimental investigation of the gabbro-eclogite transformation and some geophysical implications. *Tectonophysics* **3**, 383—427 (1966).
- RUBEY, W. W.: Geologic history of sea water. *Bull. Geol. Soc. Am.* **62**, 1111—1147 (1951).
- Development of the hydrosphere and atmosphere with special reference to the probable composition of the early atmosphere. In: *Crust of the Earth* (ed. A. POLDERVAART). *Geol. Soc. Am., Spec. Papers* **62**, 631—650 (1955).
- RUCKMICK, J. C., and J. A. NOBLE: Origin of the ultramafic complex at Union Bay, southeastern Alaska. *Bull. Geol. Soc. Am.* **70**, 981—1018 (1959).

- SCHMIDT, R. G.: Petrology of the volcanic rocks, Saipan, Mariana Islands. U.S. Geol. Survey, Profess. Papers 280, 127—176 (1957).
- SHOR jr., G. G.: Structure of the Bering Sea and the Aleutian Ridge. *Marine Geol.* **1**, 213—219 (1964).
- SNYDER, G. L.: Geology of Little Sitkin Island, Alaska. U.S. Geol. Survey, Bull. 1028-H (1959).
- TAYLOR jr., H. P., and J. A. NOBLE: Origin of the ultramafic complexes in south-eastern Alaska. Rept. 21st Sess. Internat. Geol. Congr. **13**, 175—187 (1960).
- TAYLOR, S. R., and A. J. R. WHITE: Geochemistry of andesites and the growth of continents. *Nature* **208**, 271—273 (1965).
- — Trace element abundances in andesites. *Bull. volcanol.* **29**, 177—194 (1966).
- THAYER, T. P.: Petrology of later Tertiary and Quaternary rocks of the north central Cascade Mountains in Oregon. *Bull. Geol. Soc. Am.* **48**, 1611—1652 (1937).
- TILLEY, C. E.: Some aspects of magmatic evolution. *Quart. J. Geol. Soc. London* **106**, 37—61 (1950).
- TURNER, F. J., and J. VERHOOGEN: *Igneous and metamorphic petrology*. New York: McGraw-Hill Book Co. 1960.
- TUTTLE, O. F., and N. L. BOWEN: Origin of granite in the light of experimental studies in the system $\text{NaAlSi}_3\text{O}_8 - \text{KAlSi}_3\text{O}_8 - \text{SiO}_2 - \text{H}_2\text{O}$. *Geol. Soc. Am., Mem.* **74** (1958).
- VERHOOGEN, J.: Mount St. Helens, a Recent Cascade volcano. *Calif. Univ. Dept. Geol. Sci., Bull.* **24**, 263—302 (1937).
- WAGER, L. R.: The major element variation of the layered series of the Skaergaard intrusion and a re-estimation of the average composition of the hidden layered series and of the successive residual magmas. *J. Petrology* **1**, 364—398 (1960).
- , and R. L. MITCHELL: The distribution of trace elements during strong fractionation of basic magma: a further study of the Skaergaard intrusion, East Greenland. *Geochim. et Cosmochim. Acta* **1**, 129—208 (1951).
- WATERS, A. C.: Volcanic rocks and the tectonic cycle. In: *Crust of the Earth* (ed. A. POLDERVAART). *Geol. Soc. Am., Spec. Papers* **62**, 703—722 (1955).
- WILCOX, R. E.: Petrology of Paricutin Volcano, Mexico. U.S. Geol. Survey, Bull. 965-C (1954).
- WILKINSON, J. F. G.: Some aspects of calc-alkali rock genesis. *J. Proc. Roy. Soc. N.S. Wales* **99**, 69—77 (1966).
- R. H. VERNON and S. E. SHAW: The petrology of an adamellite-porphyrite from the New England Batholith (New South Wales). *J. Petrology* **5**, 461—488 (1964).
- WILLIAMS, H.: Geology of the Lassen Volcanic National Park, California. *Calif. Univ., Dept. Geol. Sci., Bull.* **21**, 195—385 (1932).
- Mt. Shasta, California. *Zeit. Vulk.* **15**, 225—253 (1934).
- Newberry Volcano of Central Oregon. *Bull. Geol. Soc. Am.* **4—6**, 253—304 (1935).
- The geology of Crater Lake National Park, Oregon. *Carnegie Inst. Wash. Publ.* **540** (1942).
- Volcanoes of the Paricutin Region, Mexico. U.S. Geol. Survey, Bull. 965B (1950).
- F. J. TURNER and C. M. GILBERT: *Petrography*. San Francisco: W. H. Freeman and Co. 1958.
- WILSON, J. T.: The development and structure of the crust. In: *The Earth as a Planet* (ed. G. P. KUIPER), pp. 138—214. Chicago: Univ. Chicago Press 1954.
- YODER jr., H. S.: Experimental studies bearing on anorthosites. *Abst. in Symposium: Origin of Anorthosite* (ed. Y. ISACHSEN), p. 22. Plattsburgh, New York: State Univ. N.Y. 1966.
- , and C. E. TILLEY: Origin of basalt magmas: an experimental study of natural and synthetic rock systems. *J. Petrology* **3**, 342—532 (1962).

Professor A. E. RINGWOOD
Dept. of Geophysics and Geochemistry
Australian National University
Canberra, A.C.T. Australia

Dr. T. H. GREEN
Hoffman Laboratory
Harvard University
20, Oxford Street
Cambridge, Massachusetts 02138, USA